EUROPEAN ORGANIZATION FOR PARTICLE PHYSICS

LEPEWWG/97-02
ALEPH 97-085 PHYSIC 97-075
DELPHI 97-141 PHYS 726
L3 Note 2153
OPAL Technical Note TN 504
SLD Physics Note 63
18 August 1997

A Combination of Preliminary Electroweak Measurements and Constraints on the Standard Model

Internal Note

The LEP Collaborations* ALEPH, DELPHI, L3, OPAL,
the LEP Electroweak Working Group†
and the SLD Heavy Flavour Group‡

Prepared from Contributions
of the LEP and SLD experiments to the 1997 summer conferences.

Abstract

This note presents a combination of published and preliminary electroweak results from the four LEP collaborations and the SLD collaboration which were prepared for the 1997 summer conferences. Averages of the results concerning electroweak physics are presented. They are derived from the measurements of hadronic and leptonic cross sections, the leptonic forward-backward asymmetries, the τ polarisation asymmetries, the $b\overline{b}$ and $c\overline{c}$ partial widths and forward-backward asymmetries and the $q\overline{q}$ charge asymmetry. The major changes with respect to results presented last year are updated results of A_{LR} from SLD, and the inclusion of the first direct measurements of the W mass performed at LEP. The results are compared to precise electroweak measurements from other experiments. The parameters of the Standard Model are evaluated, first using the combined LEP electroweak measurements, and then using the full set of precise electroweak results.

*The LEP Collaborations each take responsibility for the preliminary data of their own experiment.

†Contact: R. Clare (Robert.Clare@cern.ch).
‡Contact: D. Su (sudong@slac.stanford.edu).

1 Introduction

The four LEP experiments have previously presented [1] parameters derived from the Z resonance using published and preliminary results based on data recorded until the end of 1995. These results represented the status of the analyses in summer 1996.

Since then a few additional preliminary results have become available. To allow a quick assessment, a box highlighting the updates is given at the beginning of each section. During 1996 LEP ran at energies of 161 and 172 GeV, allowing the production of W boson pairs for the first time in high energy e^+e^- collisions. Using these data the mass of the W boson has been measured and these new results are included in this note (where necessary these results are denoted as LEP-II). Non-W cross-section and asymmetry results from the 1996 data are reported elsewhere [2].

The LEP-I data (1990-1995) consist of the hadronic and leptonic cross sections, the leptonic forward-backward asymmetries, the τ polarisation asymmetries, the $b\overline{b}$ and $c\overline{c}$ partial widths and forward-backward asymmetries and the $q\overline{q}$ charge asymmetry. In addition, the measurements of the $b\overline{b}$ and $c\overline{c}$ partial widths and left-right-forward-backward asymmetries for b and c quarks from SLD are treated consistently with the LEP data. Many technical aspects of their combination have already been described in References 3, 4 and references therein. It should be stressed that several measurements included in the current combination are still preliminary.

This note is organised in the following manner:

Section 2 Z line shape and leptonic forward-backward asymmetries;

Section 3 τ polarisation;

Section 4 Heavy flavour analyses;

Section 5 Inclusive hadronic charge asymmetry;

Section 6 Determination of m_{W} at LEP;

Section 7 Interpretation of the results, including the combination of results from LEP, SLD, neutrino interaction experiments and from CDF and DØ;

Section 8 Prospects for the Future.

2 Z Lineshape and Lepton Forward-Backward Asymmetries

Updates from last year:
ALEPH have made significant changes in their analysis, especially for data taken in earlier years. The results from DELPHI have been updated to include the analysis of the muon and tau pair data recorded in 1995 and improvements to the analysis of the 1994 tau pair data. The L3 results are unchanged. The results from OPAL have been updated to include the hadronic cross-sections measured during the 1995 energy scan and the experimental systematic uncertainties have also been reduced. In addition, ALEPH and DELPHI have used the most recent determination of the LEP energy and errors; L3 and OPAL have evaluated the effect of the energies on their results.

The 1995 energy scan resulted in each experiment collecting approximately 40 pb^{-1} of data, of which 18 pb^{-1} was recorded at two off-peak points with centre-of-mass energies, $\sqrt{s}$, 1.8 GeV above and below the Z peak. This almost doubled the data available for precision measurements of m_{Z} and Γ_{Z}.

The results presented here are based on these new data combined with those recorded in previous years. This includes the data taken during the energy scans in 1990 and 1991 in the range $|\sqrt{s} - m_{\mathrm{Z}}| <$ 3 GeV, the data collected at the Z peak in 1992 and preliminary analyses of the energy scan in 1993 ($|\sqrt{s} - m_{\mathrm{Z}}| < 1.8$ GeV) and the peak running in 1994. The total statistics and the systematic errors on the individual analyses of the four LEP collaborations are given in Tables 1 and 2. Details of the individual analyses can be found in References 5–8.

		ALEPH	DELPHI	L3	OPAL	LEP
$\mathrm{q\overline{q}}$	'90-'91	451	357	416	454	1678
	'92	680	697	678	733	2788
	'93 prel.	640	677	646	646	2609
	'94 prel.	1654	1241	1307	1524	5726
	'95 prel.	739	584	311	344	1978
	total	4164	3556	3358	3701	14779
$\ell^+\ell^-$	'90-'91	55	36	40	58	189
	'92	82	70	58	88	298
	'93 prel.	78	74	64	82	298
	'94 prel.	190	135	127	184	630
	'95 prel.	80	67	28	42	217
	total	485	382	317	454	1638

Table 1: The LEP statistics in units of 10^3 events used for the analysis of the Z line shape and lepton forward-backward asymmetries. Not all experiments have used the full 1995 data set for the present results, in particular this applies to the data recorded before the start of the high precision energy scan.

	ALEPH			DELPHI			L3			OPAL		
	'93 prel.	'94 prel.	'95 prel.	'93 prel.	'94 prel.	'95 prel.	'93 prel.	'94 prel.	'95 prel.	'93 prel.	'94 prel.	'95 prel.
$\mathcal{L}^{\mathrm{exp.}\ (b)}$	0.067%	0.073%	0.080%	0.24%	0.09%	0.09%	0.10%	0.078%	0.128%	0.046%	0.046%	0.046%
σ_{had}	0.068%	0.072%	0.073%	0.10%	0.10%	0.10%	0.052%	0.051%	0.10%	0.084%	0.084%	0.094%
σ_{e}	0.30%	0.30%	0.31%	0.59%	0.54%	0.75%	0.30%	0.23%	1.0%	0.23%	0.24%	$^{(a)}$
σ_{μ}	0.12%	0.12%	0.12%	0.28%	0.30%	0.40%	0.31%	0.31%	1.0%	0.16%	0.15%	$^{(a)}$
σ_{τ}	0.20%	0.20%	0.20%	0.60%	0.60%	0.60%	0.67%	0.65%	0.60%	0.43%	0.46%	$^{(a)}$
$A_{\mathrm{FB}}^{\mathrm{e}}$	0.0018	0.0019	0.0020	0.0025	0.0022	0.0021	0.003	0.003	0.01	0.0016	0.0016	0.002
A_{FB}^{μ}	0.0005	0.0005	0.0005	0.0010	0.0015	0.0015	0.0008	0.0008	0.005	0.001	0.001	0.001
A_{FB}^{τ}	0.0009	0.0007	0.0009	0.0020	0.0020	0.0020	0.003	0.003	0.003	0.002	0.002	0.002

Table 2: The experimental systematic errors for the analysis of the Z line shape and lepton forward-backward asymmetries at the Z peak. The errors quoted do not include the common uncertainty due to the LEP energy calibration. The treatment of correlations between the errors for different years is described in References 5–8.

$^{(a)}$No preliminary result quoted yet.

$^{(b)}$In addition, there is a theoretical error for the calculation of the small angle Bhabha cross section of 0.11% [9], which has been treated as common to all experiments. For the present, the previous error of 0.16% [10] is used by DELPHI for 1993.

The measurement of the LEP beam energies, and the associated uncertainties, are important in

the determination of the mass and width of the Z. In this note the treatment of LEP energies is unchanged with respect to [1].

For the averaging of results the LEP experiments provide a standard set of 9 parameters describing the information contained in hadronic and leptonic cross sections and leptonic forward-backward asymmetries [3, 11]. These parameters have been corrected [12] for the effects of initial-state radiation as well as t-channel and s/t-interference in the case of e^+e^- final states. They are convenient for fitting and averaging since they have small correlations. The parameters are:

- The mass and total width of the Z boson, where the definition is based on the Breit-Wigner denominator $(s - m_Z^2 + is\Gamma_Z/m_Z)$ [12].
- The hadronic pole cross section of Z exchange:

$$\sigma_h^0 \equiv \frac{12\pi}{m_Z^2}\frac{\Gamma_{ee}\Gamma_{had}}{\Gamma_Z^2}\,.$$

  Here Γ_{ee} and Γ_{had} are the partial widths of the Z for decays into electrons and hadrons.
- The ratios:

$$R_e \equiv \Gamma_{had}/\Gamma_{ee}, \quad R_\mu \equiv \Gamma_{had}/\Gamma_{\mu\mu} \text{ and } R_\tau \equiv \Gamma_{had}/\Gamma_{\tau\tau}. \tag{1}$$

  Here $\Gamma_{\mu\mu}$ and $\Gamma_{\tau\tau}$ are the partial widths of the Z for the decays $Z \to \mu^+\mu^-$ and $Z \to \tau^+\tau^-$. Even under the assumption of lepton universality a small difference of 0.2% is expected between the values for R_e and R_μ, and the value for R_τ, owing to mass corrections to $\Gamma_{\tau\tau}$.
- The pole asymmetries, $A_{FB}^{0,e}$, $A_{FB}^{0,\mu}$ and $A_{FB}^{0,\tau}$, for the processes $e^+e^- \to e^+e^-$, $e^+e^- \to \mu^+\mu^-$ and $e^+e^- \to \tau^+\tau^-$. In terms of the effective vector and axial-vector neutral current couplings of fermions, g_{Vf} and g_{Af}, the pole asymmetries are expressed as:[1]

$$A_{FB}^{0,f} \equiv \frac{3}{4}\mathcal{A}_e\mathcal{A}_f \tag{2}$$

  with:

$$\mathcal{A}_f \equiv \frac{2g_{Vf}g_{Af}}{g_{Vf}^2 + g_{Af}^2}\,. \tag{3}$$

This set of 9 parameters does not describe the Z production and decay completely, because it does not include the interference of the Z exchange with the γ exchange. This contribution is investigated in a separate note [2]. For the results presented in this note, the γ-exchange contributions and the γZ interference terms are fixed to their Standard Model values.[2]

The four sets of 9 parameters provided by the LEP experiments are presented in Table 3. The covariance matrix of these parameters is constructed as described in Reference 11. It is constructed from the covariance matrices of the individual LEP experiments and common systematic errors. These common errors arise from the theoretical uncertainty in the luminosity normalisation affecting the hadronic pole cross section, $\Delta\sigma_h^0/\sigma_h^0 = 0.11\%$, from the uncertainty of the LEP centre-of-mass energy spread of about 1 MeV [13], resulting in $\Delta\Gamma_Z \approx 0.2$ MeV, and from the uncertainty in the LEP energy calibration. The latter uncertainty causes errors of $\Delta m_Z \approx 1.5$ MeV and $\Delta\Gamma_Z \approx 1.5$ MeV [14]. The combined parameter set and its correlation matrix are given in Tables 4 and 5.

[1] In the definition of $A_{FB}^{0,f}$, effects from γ exchange, γ/Z interference, as well as real and imaginary parts of the photon vacuum polarisation, are not included. They are accounted for explicitly in the fitting formulae used by the experiments, and are fixed to their Standard Model values.

[2] If instead the γZ interference terms are entirely determined from LEP cross-section data (including the 130-172 GeV data), the total error on the LEP average of m_Z increases from 2.0 MeV to 3.1 MeV [2].

	ALEPH	DELPHI	L3[a]	OPAL[b]
$m_{\rm Z}$(GeV)	91.1883±0.0031	91.1866±0.0029	91.1883±0.0029	91.1838±0.0029
$\Gamma_{\rm Z}$(GeV)	2.4951±0.0043	2.4893±0.0040	2.4996±0.0043	2.4958±0.0043
$\sigma^0_{\rm h}$(nb)	41.520±0.068	41.566±0.079	41.411±0.074	41.46±0.07
R_e	20.66±0.09	20.89±0.13	20.78±0.11	20.83±0.14
R_μ	20.82±0.06	20.69±0.08	20.84±0.10	20.79±0.07
R_τ	20.77±0.07	20.88±0.13	20.75±0.14	20.98±0.11
$A^{0,\,\rm e}_{\rm FB}$	0.0176±0.0037	0.0189±0.0050	0.0148±0.0063	0.0107±0.0054
$A^{0,\,\mu}_{\rm FB}$	0.0170±0.0025	0.0154±0.0027	0.0176±0.0035	0.0156±0.0026
$A^{0,\,\tau}_{\rm FB}$	0.0167±0.0028	0.0222±0.0039	0.0233±0.0049	0.0189±0.0034
χ^2/d.o.f.	178/177	183/162	142/159	11/6[c]

Table 3: Line shape and asymmetry parameters from 9-parameter fits to the data of the four LEP experiments.
[a] These results use the energies as given in Ref. [15]. L3 has estimated that using the new energies the mass would shift by +0.3 MeV and the width by +0.3 MeV, which have been used in subsequent fits.
[b] These results use the energies as given in Ref. [15]. OPAL has estimated that using the new energies the mass would shift by +0.5 MeV and the width by 0.0 MeV, which have been used in subsequent fits.
[c] This parameter set has been obtained from a parameter transformation applied to the 15 parameters of the OPAL fit [8], which treats the γZ interference terms for leptons as additional free parameters. The extra parameters for the γZ interference terms have been fixed to their Standard Model values in the transformation. The χ^2/d.o.f. for the 15-parameter fit to the data is 96/144.

Parameter	Average Value
$m_{\rm Z}$(GeV)	91.1867±0.0020
$\Gamma_{\rm Z}$(GeV)	2.4948±0.0025
$\sigma^0_{\rm h}$(nb)	41.486±0.053
$R_{\rm e}$	20.757±0.056
R_μ	20.783±0.037
R_τ	20.823±0.050
$A^{0,\,\rm e}_{\rm FB}$	0.0160±0.0024
$A^{0,\,\mu}_{\rm FB}$	0.0163±0.0014
$A^{0,\,\tau}_{\rm FB}$	0.0192±0.0018

Table 4: Average line shape and asymmetry parameters from the data of the four LEP experiments given in Table 3, without the assumption of lepton universality. The χ^2/d.o.f. of the average is 21/27.

	$m_{\rm Z}$	$\Gamma_{\rm Z}$	$\sigma^0_{\rm h}$	$R_{\rm e}$	R_μ	R_τ	$A^{0,\,\rm e}_{\rm FB}$	$A^{0,\,\mu}_{\rm FB}$	$A^{0,\,\tau}_{\rm FB}$
$m_{\rm Z}$	1.00	0.05	−0.01	0.00	−0.03	−0.02	.02	.05	.04
$\Gamma_{\rm Z}$		1.00	−0.16	−0.00	−0.01	−0.00	−.00	−.00	.00
$\sigma^0_{\rm h}$			1.00	0.06	0.11	0.08	.00	.00	.00
$R_{\rm e}$				1.00	0.05	0.04	−.02	.01	.00
R_μ					1.00	0.06	−.00	.01	−.00
R_τ						1.00	−.00	.00	.01
$A^{0,\,\rm e}_{\rm FB}$							1.00	.01	.01
$A^{0,\,\mu}_{\rm FB}$								1.00	.02
$A^{0,\,\tau}_{\rm FB}$									1.00

Table 5: The correlation matrix for the set of parameters given in Table 4.

The estimation of the common errors mentioned above which arise from the LEP energy calibration is more complicated than in previous years due to the correlations in the LEP energy error matrix between the 1993 and 1995 scans. The procedure adopted is the same approximate method as has been used for the previous note. Two fits are performed to a data set from a single experiment. The first is a normal fit, whereas in the second fit all errors except those due to the LEP energy uncertainty are halved. The procedure results in two covariance matrices, $V_1 = V_E + V_O$ and $V_2 = V_E + V_O/4$, where V_E contains the components due to energy, and V_O contains all other components. V_E is obtained algebraically from V_1 and V_2, and is then used as a correlated part of the full covariance matrix when combining the data from experiments. The result [3] is insensitive to which of the experiments is used to provide the data.

If lepton universality is assumed, the set of 9 parameters given above is reduced to a set of 5 parameters. R_ℓ is defined as $R_\ell \equiv \Gamma_{\rm had}/\Gamma_{\ell\ell}$, where $\Gamma_{\ell\ell}$ refers to the partial Z width for the decay into a pair of massless charged leptons. The data of each of the four LEP experiments are consistent with lepton universality (the difference in χ^2 over the difference in d.o.f. with and without the assumption of lepton universality is 4/4, 4/4, 2/4 and 3/4 for ALEPH, DELPHI, L3 and OPAL, respectively). Table 6 gives the five parameters $m_{\rm Z}$, $\Gamma_{\rm Z}$, $\sigma^0_{\rm h}$, R_ℓ and $A^{0,\ell}_{\rm FB}$ for the individual LEP experiments, assuming lepton universality. Tables 7 and 8 give the combined result and the corresponding correlation matrix. Figure 1 shows, for each lepton species and for the combination assuming lepton universality, the resulting 68% probability contours in the R_ℓ-$A^{0,\ell}_{\rm FB}$ plane. For completeness the partial decay widths of the Z boson are listed in Table 9.

[3] This procedure was previously checked [1] by performing a global fit to the hadronic cross-section data for all experiments for the years 1993, 1994 and 1995. This procedure included all common errors without any approximations being necessary, and was therefore exact apart from the fact the data from earlier years and the leptonic channels were not used. The results agreed with those of the method described in the text.

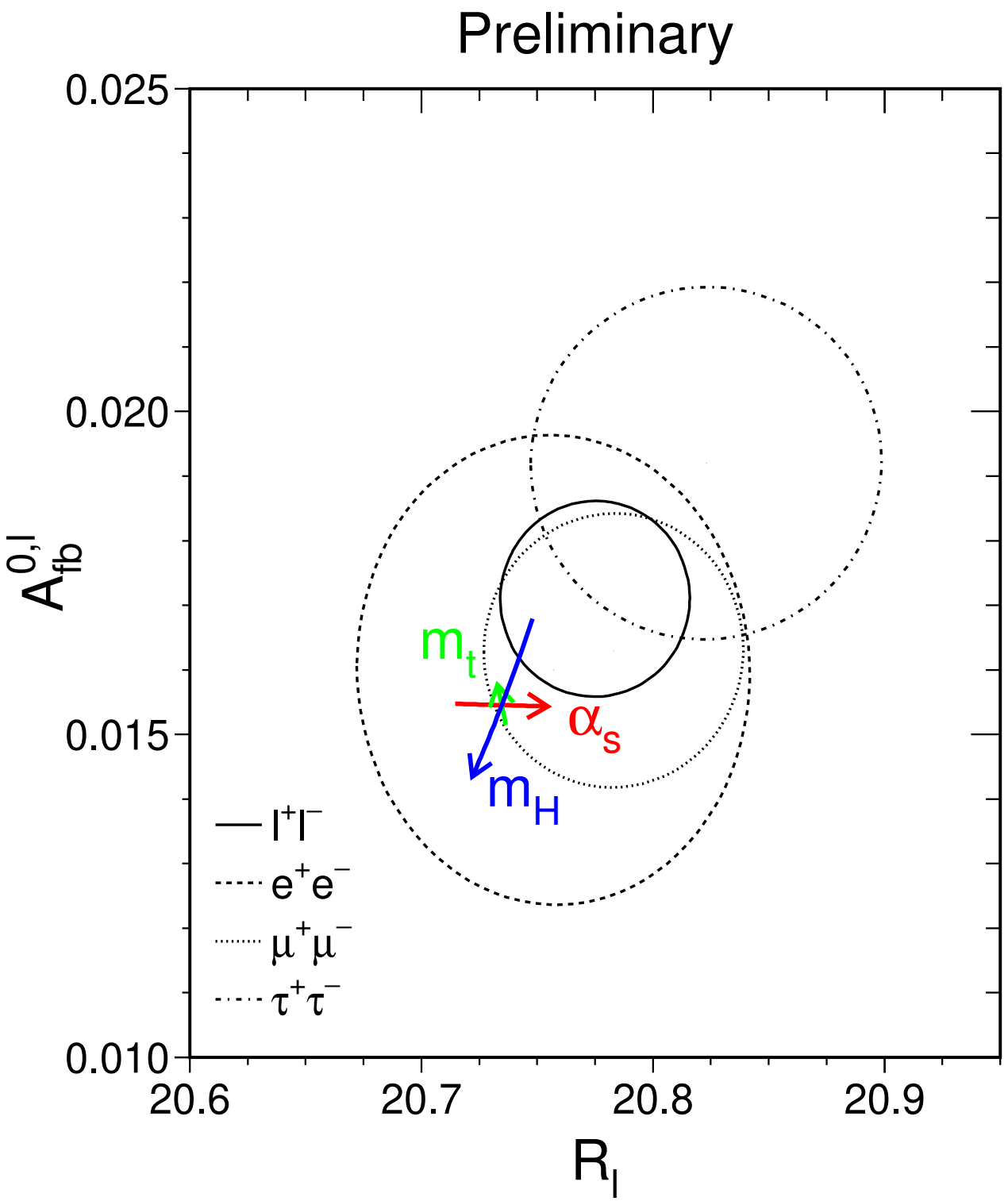

Figure 1: Contours of 68% probability in the R_ℓ-$A_{\rm FB}^{0,\ell}$ plane. The Standard Model prediction for $m_{\rm Z} = 91.1867$ GeV, $m_{\rm t} = 175.6$ GeV, $m_{\rm H} = 300$ GeV, and $\alpha_s(m_{\rm Z}^2) = 0.118$ is also shown. The lines with arrows correspond to the variation of the Standard Model prediction when $m_{\rm t}$, $m_{\rm H}$ or $\alpha_s(m_{\rm Z}^2)$ are varied in the intervals $m_{\rm t} = 175.6 \pm 5.5$ GeV, $m_{\rm H} = 300^{+700}_{-240}$ GeV, and $\alpha_s(m_{\rm Z}^2) = 0.118 \pm 0.003$, respectively. The arrows point in the direction of increasing values of $m_{\rm t}$, $m_{\rm H}$ and α_s.

	ALEPH	DELPHI	L3	OPAL
$m_{\rm Z}$(GeV)	91.1883±0.0031	91.1866±0.0029	91.1883±0.0029	91.1836±0.0029
$\Gamma_{\rm Z}$(GeV)	2.4951±0.0043	2.4893±0.0040	2.4996±0.0043	2.4958±0.0043
$\sigma^0_{\rm h}$(nb)	41.520±0.068	41.557±0.079	41.411±0.074	41.456±0.071
R_ℓ	20.754±0.043	20.759±0.062	20.788±0.066	20.834±0.056
$A^{0,\ell}_{\rm FB}$	0.0170±0.0017	0.0178±0.0021	0.0187±0.0026	0.0160±0.0019
χ^2/d.o.f.	182/181	187/166	144/163	14/10[(c)]

Table 6: Line shape and asymmetry parameters from 5-parameter fits to the data of the four LEP experiments, assuming lepton universality. R_ℓ is defined as $R_\ell \equiv \Gamma_{\rm had}/\Gamma_{\ell\ell}$, where $\Gamma_{\ell\ell}$ refers to the partial Z width for the decay into a pair of massless charged leptons.
[(a)] These results use the energies as given in Ref. [15]. L3 has estimated that using the new energies the mass would shift by +0.3 MeV and the width by +0.3 MeV, which have been used in subsequent fits.
[(b)] These results use the energies as given in Ref. [15]. OPAL has estimated that using the new energies the mass would shift by +0.5 MeV and the width by 0.0 MeV, which have been used in subsequent fits.
[(c)] This parameter set has been obtained by a parameter transformation applied to the 15 parameters of the OPAL fit.

Parameter	Average Value
$m_{\rm Z}$(GeV)	91.1867±0.0020
$\Gamma_{\rm Z}$(GeV)	2.4948±0.0025
$\sigma^0_{\rm h}$(nb)	41.486±0.053
R_ℓ	20.775±0.027
$A^{0,\ell}_{\rm FB}$	0.0171±0.0010

Table 7: Average line shape and asymmetry parameters from the results of the four LEP experiments given in Table 6, assuming lepton universality. R_ℓ is defined as $R_\ell \equiv \Gamma_{\rm had}/\Gamma_{\ell\ell}$, where $\Gamma_{\ell\ell}$ refers to the partial Z width for the decay into a pair of massless charged leptons. The χ^2/d.o.f. of the average is 23/31.

	$m_{\rm Z}$	$\Gamma_{\rm Z}$	$\sigma^0_{\rm h}$	R_ℓ	$A^{0,\ell}_{\rm FB}$
$m_{\rm Z}$	1.00	0.05	−0.01	−0.02	0.06
$\Gamma_{\rm Z}$		1.00	−0.16	−0.00	−0.00
$\sigma^0_{\rm h}$			1.00	0.14	0.00
R_ℓ				1.00	0.01
$A^{0,\ell}_{\rm FB}$					1.00

Table 8: The correlation matrix for the set of parameters given in Table 7.

Without Lepton Universality:		
$\Gamma_{\rm ee}$	(MeV)	83.94±0.14
$\Gamma_{\mu\mu}$	(MeV)	83.84±0.20
$\Gamma_{\tau\tau}$	(MeV)	83.68±0.24

With Lepton Universality:		
$\Gamma_{\ell\ell}$	(MeV)	83.91±0.10
$\Gamma_{\rm had}$	(MeV)	1743.2±2.3
$\Gamma_{\rm inv}$	(MeV)	500.1±1.8

Table 9: Partial decay widths of the Z boson, derived from the results of the 9-parameter (Tables 4 and 5) and the 5-parameter fit (Tables 7 and 8). In the case of lepton universality, $\Gamma_{\ell\ell}$ refers to the partial Z width for the decay into a pair of massless charged leptons.

3 The τ Polarisation

Updates from last year:
L3 has reanalysed their 1994 data and have included the 1995 data.

The τ polarisation, $\mathcal{P}_\tau$, is determined by a measurement of the longitudinal polarisation of τ pairs produced in Z decays. It is defined as:

$$\mathcal{P}_\tau \equiv \frac{\sigma_R - \sigma_L}{\sigma_R + \sigma_L}\,, \tag{4}$$

where σ_R and σ_L are the τ-pair cross sections for the production of a right-handed and left-handed τ^-, respectively. The angular distribution of $\mathcal{P}_\tau$ as a function of the angle θ between the e^- and the τ^-, for $\sqrt{s} = m_Z$, is given by:

$$\mathcal{P}_\tau(\cos\theta) = -\frac{\mathcal{A}_\tau(1+\cos^2\theta) + 2\mathcal{A}_e\cos\theta}{1+\cos^2\theta + 2\mathcal{A}_\tau\mathcal{A}_e\cos\theta}\,, \tag{5}$$

with $\mathcal{A}_e$ and $\mathcal{A}_\tau$ as defined in Equation (3). Equation (5) neglects corrections for the effects of γ exchange, γZ interference and electromagnetic radiative corrections for initial- and final-state radiation. These effects are taken into account in the experimental analyses. In particular, these corrections account for the $\sqrt{s}$ dependence of the tau polarisation, $\mathcal{P}_\tau(\cos\theta)$, which is important since the off-peak data are included in the event samples for all experiments. When averaged over all production angles $\mathcal{P}_\tau$ is a measurement of $\mathcal{A}_\tau$. As a function of $\cos\theta$, $\mathcal{P}_\tau(\cos\theta)$ provides nearly independent determinations of both $\mathcal{A}_\tau$ and $\mathcal{A}_e$, thus allowing a test of the universality of the couplings of the Z to e and τ.

Each experiment makes separate $\mathcal{P}_\tau$ measurements using the five τ decay modes $e\nu\overline{\nu}$, $\mu\nu\overline{\nu}$, $\pi\nu$, $\rho\nu$ and $a_1\nu$ [16–19]. The $\rho\nu$ and $\pi\nu$ are the most sensitive channels, contributing weights of about 40% each in the average. DELPHI has also used an inclusive hadronic analysis. The combination is made of the results from each experiment already averaged over the τ decay modes.

3.1 Results

Tables 10 and 11 show the most recent results for $\mathcal{A}_\tau$ and $\mathcal{A}_e$ obtained by the four experiments [16–19] and their combination. A study of the possible common systematic errors has shown these to be small [3] and thus no such errors have been included in the combination. The statistical correlation between the extracted values of $\mathcal{A}_\tau$ and $\mathcal{A}_e$ is small ($\leq 5\%$), and is neglected.

The average values for $\mathcal{A}_\tau$ and $\mathcal{A}_e$:

$$\mathcal{A}_\tau = 0.1410 \pm 0.0064 \tag{6}$$
$$\mathcal{A}_e = 0.1399 \pm 0.0073\,, \tag{7}$$

are compatible, as is expected from lepton universality. Assuming $e-\tau$ universality, the values for $\mathcal{A}_\tau$ and $\mathcal{A}_e$ can be combined. This combination is performed neglecting any possible common systematic error between $\mathcal{A}_\tau$ and $\mathcal{A}_e$ within a given experiment, as these errors are also estimated to be small. The combined result of $\mathcal{A}_\tau$ and $\mathcal{A}_e$ gives:

$$\mathcal{A}_\ell = 0.1406 \pm 0.0048\,. \tag{8}$$

ALEPH	('90 - '92), final	$0.136 \pm 0.012 \pm 0.009$
DELPHI	('90 - '94), prel.	$0.138 \pm 0.009 \pm 0.008$
L3	('90 - '95), prel.	$0.152 \pm 0.010 \pm 0.006$
OPAL	('90 - '94), final	$0.134 \pm 0.009 \pm 0.010$
LEP Average		0.1410 ± 0.0064

Table 10: LEP results for $\mathcal{A}_\tau$. The χ^2/d.o.f. for the average is 1.4/3. The first error is statistical and the second systematic. In the LEP average, statistical and systematic errors are combined in quadrature. The systematic component of the error, obtained by combining the individual systematic errors (weighted by the total errors), is ± 0.0040.

ALEPH	('90 - '92), final	$0.129 \pm 0.016 \pm 0.005$
DELPHI	('90 - '94), prel.	$0.140 \pm 0.013 \pm 0.003$
L3	('90 - '95), prel.	$0.158 \pm 0.014 \pm 0.004$
OPAL	('90 - '94), final	$0.129 \pm 0.014 \pm 0.005$
LEP Average		0.1399 ± 0.0073

Table 11: LEP results for $\mathcal{A}_e$. The χ^2/d.o.f. for the average is 2.4/3. The first error is statistical and the second systematic. In the LEP average, statistical and systematic errors are combined in quadrature. The systematic component of the error, obtained by combining the individual systematic errors (weighted by the total errors), is ± 0.0020.

4 Results from b and c Quarks

Updates from last year:
Several new results on R_b are available. The $\mathcal{A}_c$ measurement of SLD has improved significantly and several other measurements have been updated.

The relevant quantities in the heavy quark sector at LEP which are currently determined by the combination procedure are:

- The ratios[4] of the b and c quark partial widths of the Z to its total hadronic partial width: $R_b^0 \equiv \Gamma_{b\bar{b}}/\Gamma_{had}$ and $R_c^0 \equiv \Gamma_{c\bar{c}}/\Gamma_{had}$.
- The forward-backward asymmetries, $A_{FB}^{b\bar{b}}$ and $A_{FB}^{c\bar{c}}$.
- The semileptonic branching ratios, $BR(b \to \ell)$ and $BR(b \to c \to \bar{\ell})$, and the average $B^0\overline{B^0}$ mixing parameter, $\overline{\chi}$. These are often determined at the same time as the widths or asymmetries in multi-parameter fits to lepton tag samples. They are included in the combination procedure to take into account their correlations with the other parameters measured in the same fit.
- The probability that a c-quark produces a D^{*+}[5], a D^+, a D_s or a charmed baryon. The probability that a c-quark fragments into a D^0 is calculated from the constraint that the probabilities for the weakly decaying charmed hadrons add up to one. These quantities are determined now with good accuracy by the LEP experiments. The interpretation of the D^* rate in terms of R_c and the determination of the charm background in the lifetime tag R_b measurements can now be made without assumptions on the energy dependence of the D-meson production rates.

There are several motivations for the averaging procedure [4] presented here. Several analyses measure more than one parameter simultaneously, for example the lepton fits. Some of the measurements of electroweak parameters depend explicitly on the values of other parameters, for example R_b depends on R_c. The common tagging and analysis techniques lead to common sources of systematic uncertainty, in particular for the double-tag measurements of R_b. The starting point for the combination is to ensure that all the analyses use a common set of assumptions for input parameters which give rise to systematic uncertainties. A full description of the averaging procedure has been published in Reference 4. The input parameters have been updated and extended recently [20] to accommodate new analyses and more recent measurements. The correlations and interdependences of the input measurements are then taken into account in a χ^2 minimisation which results in the combined electroweak parameters and their correlation matrix.

In a first fit the asymmetry measurements on peak, above peak and below peak were combined at each centre-of-mass energy. The results of this fit, including the SLD results, are given in the appendix. The dependence of the average asymmetries on centre-of-mass energy agrees with the prediction of the Standard Model. To derive the pole asymmetries, $A_{FB}^{0,q}$, from the measured quark asymmetries, all the off-peak asymmetry measurements were corrected to the peak energy before combining. Only results from this second fit are quoted here. There are therefore 11 parameters in total to be determined: the two partial widths, two asymmetries, two semileptonic branching ratios, the average mixing parameter and the probabilities for c quark to fragment into a D^{*+}, a D^+ a D_s, or a charmed baryon.

[4] The symbols R_b^0, R_c^0 denote the ratio of partial widths whereas R_b, R_c denote the experimentally measured ratios of cross sections ($R_b^0 = R_b + 0.0003$, $R_c^0 = R_c - 0.0003$).

[5] Actually the product $P(c \to D^{*+}) \times BR(D^{*+} \to \pi^+ D^0)$ is fitted since this quantity is needed and measured by the LEP experiments.

In addition the SLD collaboration has presented precise measurements of $R_{\rm b}$ [21], $R_{\rm c}$ [22] and of the left-right forward-backward asymmetry for b and c quarks [23]. Since the precision and the dominant sources of systematic uncertainty are similar at LEP and SLD it is useful to produce combined LEP+SLD averages. The left-right forward-backward asymmetries are, in contrast to the unpolarised forward-backward asymmetries, only sensitive to the final state couplings ($\mathcal{A}_{\rm b}$ and $\mathcal{A}_{\rm c}$). They are treated in the averaging procedure as physically independent quantities. However the methods used to measure the polarised and unpolarised asymmetries are very similar, so $\mathcal{A}_{\rm b}$ and $\mathcal{A}_{\rm c}$ are included in the averaging procedure in order to estimate the correlation between the SLD and the LEP asymmetries, resulting in a 13-parameter fit.

4.1 Summary of measurements and averaging procedure

The measurements of $R_{\rm b}$ and $R_{\rm c}$ fall into two categories. In the first, called a single-tag measurement, a method to select b or c events is devised, and the number of tagged events is counted. This number must then be corrected for backgrounds from other flavours and for the tagging efficiency to calculate the true fraction of hadronic Z decays of that flavour. The dominant systematic errors come from understanding the branching ratios and detection efficiencies which give the overall tagging efficiency. For the second technique, called a double-tag measurement, the event is divided into two hemispheres. With N_t being the number of tagged hemispheres, N_{tt} the number of events with both hemispheres tagged and $N_{\rm had}$ the total number of hadronic Z decays one has:

$$\begin{aligned} \frac{N_t}{2N_{\rm had}} &= \varepsilon_{\rm b}R_{\rm b} + \varepsilon_{\rm c}R_{\rm c} + \varepsilon_{\rm uds}(1 - R_{\rm b} - R_{\rm c}), \\ \frac{N_{tt}}{N_{\rm had}} &= \mathcal{C}_{\rm b}\varepsilon_{\rm b}^2 R_{\rm b} + \mathcal{C}_{\rm c}\varepsilon_{\rm c}^2 R_{\rm c} + \mathcal{C}_{\rm uds}\varepsilon_{\rm uds}^2(1 - R_{\rm b} - R_{\rm c}), \end{aligned}$$

where $\varepsilon_{\rm b}$, $\varepsilon_{\rm c}$ and $\varepsilon_{\rm uds}$ are the tagging efficiencies per hemisphere for b, c and light-quark events, and $\mathcal{C}_{\rm q} \neq 1$ accounts for the fact that the tagging efficiencies between the hemispheres may be correlated. In the case of $R_{\rm b}$ one has $\varepsilon_{\rm b} \gg \varepsilon_{\rm c} \gg \varepsilon_{\rm uds}$, $\mathcal{C}_{\rm b} \approx 1$. The correlations for the other flavours can be neglected. These equations can be solved to give $R_{\rm b}$ and $\varepsilon_{\rm b}$. Neglecting the c and uds backgrounds and the correlations they are approximately given by:

$$\begin{aligned} \varepsilon_{\rm b} &\approx 2N_{tt}/N_t, \\ R_{\rm b} &\approx N_t^2/(4N_{tt}N_{\rm had}). \end{aligned}$$

The double-tagging method has the advantage that the b tagging efficiency is derived directly from the data, reducing the systematic error of the measurement. The residual background of other flavours in the sample, and the evaluation of the correlation between the tagging efficiencies in the two hemispheres of the event are the main sources of systematic uncertainty in such an analysis.

The measurements included are:

- Lepton fits from all four LEP experiments [24–29]. These analyses use hadronic events with one or more leptons in the final state. Each analysis fits for several parameters chosen from $R_{\rm b}$, $R_{\rm c}$, $A_{\rm FB}^{\rm b\bar{b}}$, $A_{\rm FB}^{\rm c\bar{c}}$, BR($\rm b \to \ell$) and BR($\rm b \to c \to \bar{\ell}$), and $\overline{\chi}$. Correlations exist between the different measured quantities, especially between $R_{\rm b}$ and BR($\rm b \to \ell$). $R_{\rm b}$ and the semileptonic branching ratios are measured by a double-tagging technique where for the branching ratios the lepton identification efficiency needs to be known. The dominant sources of systematic error for the lepton fits arise from the lepton identification, from other semileptonic branching ratios and from the modelling of the semileptonic decay. In addition to the single/double lepton fits ALEPH

and DELPHI have measured BR($b \to \ell$) and BR($b \to c \to \bar{\ell}$) in a lifetime tagged sample and ALEPH has measured R_c from low energy electrons assuming a value of BR($c \to \ell$) [24, 30].

- Event-shape tag for R_b from L3 (single tag) [31].

- Lifetime (and lepton) double tag measurements for R_b from ALEPH, DELPHI, L3, OPAL and SLD [21, 32–35]. These are the most precise determinations of R_b, and dominate the combined result. The basic features of the double-tag technique were discussed above. In the ALEPH, DELPHI and SLD measurements the charm rejection has been enhanced by using the invariant mass information where DELPHI adds also information from the energy off all particles at the secondary vertex and their rapidity. The ALEPH and DELPHI measurements make use of several different tags; this improves the statistical accuracy and reduces the systematic errors due to hemisphere correlations and charm contamination, compared to the simple single/double tag.

- Measurements of $A_{FB}^{b\bar{b}}$ based on lifetime tagged events with a hemisphere charge measurement from DELPHI, L3 and OPAL. The mean b-hemisphere charge is derived from the charge distributions themselves [27, 36, 37]. These measurements contribute roughly the same weight to the combined result as the lepton fits. The preliminary ALEPH meaurement prepared for the Warsaw conference has been withdrawn. A new publication on the entire LEP1 data set is expected very soon.

- Analyses with $D/D^{*\pm}$ mesons to measure R_c from ALEPH, DELPHI and OPAL [25, 38, 39]. All measurements are constructed in a way that no assumptions on the energy dependence of charm fragmentation are necessary. The available measurements can be divided into four groups:

  - inclusive/exclusive double tag (ALEPH, DELPHI, OPAL): In a first step $D^{*\pm}$ mesons are reconstructed in several decay channels and their production rate is measured, which depends on the product $R_c \times P(c \to D^{*+}) \times BR(D^{*+} \to \pi^+ D^0)$. This sample of clean $c\bar{c}$ (and $b\bar{b}$) events is then used to measure $P(c \to D^{*+}) \times BR(D^{*+} \to \pi^+ D^0)$ using a slow pion tag in the opposite hemisphere. In the ALEPH measurement R_c is unfolded internally in the analysis so that no explicit $P(c \to D^{*+}) \times BR(D^{*+} \to \pi^+ D^0)$ is available. However the principle of the method is identical to the one of DELPHI and OPAL.
  - inclusive single/double tag (DELPHI): This measurement measures the single and double tag rate using a slow pion tag. It takes advantage of the much higher efficiency of the inclusive slow pion tag compared to the exclusive reconstruction. The high background, however, limits the precision of this measurement.
  - exclusive double tag (ALEPH): This analysis uses exclusively reconstructed D^{*+}, D^0 and D^+ mesons in different decay channels. It has lower statistics but much better purity than the inclusive analyses.
  - Reconstruction of all weakly decaying D states (ALEPH, DELPHI, OPAL): These analyses make the assumption that the production rates of D^0, D^+, D_s and Λ_c saturate the fragmentation of $c\bar{c}$ with small corrections applied for the unobserved baryonic states. This is a single tag measurement, relying only on knowing the decay branching ratios of the charm hadrons. The DELPHI and OPAL analyses are also used to measure the c-hadron production ratios which are needed for the R_b analyses. This information is currently not used from the ALEPH analysis, however it clearly should be possible to use in future.

- A lifetime plus mass double tag from SLD to measure R_c [22]. This analysis uses the same tagging algorithm as the SLD R_b analysis however requiering that the mass of the secondary vertex is smaller than the D-meson mass. The charm tag has a purity of about 67%, however most of the background is coming from b which can be measured from the b/c mixed tag rate.

- Analyses with D mesons to measure $A_{\rm FB}^{\rm c\bar{c}}$ from ALEPH [40] or $A_{\rm FB}^{\rm c\bar{c}}$ and $A_{\rm FB}^{\rm b\bar{b}}$ from DELPHI and OPAL [27, 41].
- Measurements of $\mathcal{A}_{\rm b}$ and $\mathcal{A}_{\rm c}$ from SLD [23]. These results use lepton, kaon, D mesons and lifetime plus hemisphere charge tags, with similar sources of systematic error as the LEP asymmetry measurements.

These measurements are presented by the LEP and SLD collaborations in a consistent manner for the purpose of combination [4]. The tables prepared by the experiments include a detailed breakdown of the systematic error of each measurement and its dependence on other electroweak parameters. Where necessary, the experiments apply small corrections to their results in order to use agreed values and ranges for the input parameters to calculate systematic errors. The measurements, corrected where necessary, are summarised in the Appendix in Tables 27-40, where the statistical and systematic errors are quoted separately. The correlated systematic entries are from sources shared with one or more other results in the table and are derived from the full breakdown of common systematic uncertainties. The uncorrelated systematic entries come from the remaining sources.

A χ^2 minimisation procedure is used to derive the values of the heavy-flavour electroweak parameters as published in Reference 4. The full statistical and systematic covariance matrix for all measurements is calculated. This correlation matrix takes correlations between different measurements of one experiment and between different experiments into account. The explicit dependencies of each measurement on the other parameters are also accounted for. The most important example is the dependence of the value of $R_{\rm b}$ on the assumed value of $R_{\rm c}$.

Since c-quark events form the main background in the $R_{\rm b}$ analyses, the value of $R_{\rm b}$ depends on the value of $R_{\rm c}$. If $R_{\rm b}$ and $R_{\rm c}$ are measured in the same analysis, this is reflected in the correlation matrix for the results. However most analyses do not determine $R_{\rm b}$ and $R_{\rm c}$ simultaneously but instead measure $R_{\rm b}$ for an assumed value of $R_{\rm c}$. In this case the dependence is parametrised as:

$$R_{\rm b} = R_{\rm b}^{\rm meas} + a(R_{\rm c})\frac{(R_{\rm c} - R_{\rm c}^{\rm used})}{R_{\rm c}}. \tag{9}$$

In this expression, $R_{\rm b}^{\rm meas}$ is the result of the analysis assuming a value of $R_{\rm c} = R_{\rm c}^{\rm used}$. The values of $R_{\rm c}^{\rm used}$ and the coefficients $a(R_{\rm c})$ are given in Table 27 where appropriate. The dependences of all other measurements on other electroweak parameters are treated in the same way, with coefficients $a(x)$ describing the dependence on parameter x.

4.2 Treatment of the LEP Asymmetry Measurements

For the 11- and 13-parameter fits described above, the peak and off-peak asymmetries were corrected to $\sqrt{s} = 91.26$ GeV using the predicted dependence from ZFITTER [42]. The slope of the asymmetry around $m_{\rm Z}$ depends only on the axial coupling and the charge of the initial and final state fermions and is thus independent of the value of the asymmetry itself.

The QCD corrections to the forward-backward asymmetries depend strongly on the experimental analyses. For this reason the numbers given by the colaborations are already corrected for QCD efects. A detailed description of the applied procedure can be found in [43].

After calculating the overall averages, the quark pole asymmetries, $A_{\rm FB}^{0,\,\rm q}$, were derived by applying the corrections described below. The measured asymmetries are all corrected to full acceptance. To

relate the pole asymmetries to these numbers a few corrections that are summarised in Table 12 have to be applied. These corrections are the effects of the energy shift from 91.26 GeV to $m_{\rm Z}$, initial state radiation, and γ exchange and γZ interference. A very small correction due to the finite value of the b-quark mass is included in the correction called γZ interference. All have been calculated using ZFITTER.

Source	$\delta A_{\rm FB}^{\rm b}$	$\delta A_{\rm FB}^{\rm c}$
$\sqrt{s} = m_{\rm Z}$	-0.0013	-0.0034
QED corrections	$+0.0041$	$+0.0104$
γ, γZ	-0.0003	-0.0008
Total	$+0.0025$	$+0.0062$

Table 12: Corrections to be applied to the quark asymmetries. The corrections are to be understood as $A_{\rm FB}^0 = A_{\rm FB}^{meas} + \sum_i (\delta A_{\rm FB})_i$.

4.3 Results

4.3.1 Results of the 11-parameter fit to LEP data

Using the full averaging procedure gives the following combined results for the electroweak parameters:

$$\begin{aligned} R_{\rm b}^0 &= 0.2174 \pm 0.0009 \\ R_{\rm c}^0 &= 0.1727 \pm 0.0050 \\ A_{\rm FB}^{0,\,\rm b} &= 0.0983 \pm 0.0024 \\ A_{\rm FB}^{0,\,\rm c} &= 0.0739 \pm 0.0048\,, \end{aligned} \tag{10}$$

where all corrections to the asymmetries and partial widths have been applied. The χ^2/d.o.f. is $51/(86-11)$. The corresponding correlation matrix is given in Table 13.

	$R_{\rm b}^0$	$R_{\rm c}^0$	$A_{\rm FB}^{0,\,\rm b}$	$A_{\rm FB}^{0,\,\rm c}$
$R_{\rm b}^0$	1.00	-0.22	-0.03	0.02
$R_{\rm c}^0$	-0.22	1.00	0.03	-0.08
$A_{\rm FB}^{0,\,\rm b}$	-0.03	0.03	1.00	0.13
$A_{\rm FB}^{0,\,\rm c}$	0.02	-0.08	0.13	1.00

Table 13: The reduced correlation matrix for the electroweak parameters from the 11-parameter fit.

4.3.2 Results of the 13-parameter fit to LEP and SLD data

Including the SLD results on $R_{\rm b}$, $\mathcal{A}_{\rm b}$ and $\mathcal{A}_{\rm c}$ into the fit the following results are obtained:

$$\begin{aligned} R_{\rm b}^0 &= 0.2170 \pm 0.0009 \\ R_{\rm c}^0 &= 0.1734 \pm 0.0048 \\ A_{\rm FB}^{0,\,\rm b} &= 0.0984 \pm 0.0024 \\ A_{\rm FB}^{0,\,\rm c} &= 0.0741 \pm 0.0048 \\ \mathcal{A}_{\rm b} &= 0.900 \pm 0.050 \\ \mathcal{A}_{\rm c} &= 0.650 \pm 0.058\,, \end{aligned} \tag{11}$$

with a χ^2/d.o.f. of $53/(94-13)$. The corresponding correlation matrix is given in Table 14. In deriving these results the parameters $\mathcal{A}_{\rm b}$ and $\mathcal{A}_{\rm c}$ have been treated as independent of the forward-backward asymmetries $A_{\rm FB}^{\rm b\bar{b}}({\rm pk})$ and $A_{\rm FB}^{\rm c\bar{c}}({\rm pk})$.

	$R_{\rm b}^0$	$R_{\rm c}^0$	$A_{\rm FB}^{0,\,{\rm b}}$	$A_{\rm FB}^{0,\,{\rm c}}$	$\mathcal{A}_{\rm b}$	$\mathcal{A}_{\rm c}$
$R_{\rm b}^0$	1.00	-0.20	-0.03	0.01	-0.03	0.02
$R_{\rm c}^0$	-0.20	1.00	0.03	-0.07	0.04	-0.04
$A_{\rm FB}^{0,\,{\rm b}}$	-0.03	0.03	1.00	0.13	0.03	0.02
$A_{\rm FB}^{0,\,{\rm c}}$	0.01	-0.07	0.13	1.00	0.00	0.07
$\mathcal{A}_{\rm b}$	-0.03	0.04	0.03	0.00	1.00	0.08
$\mathcal{A}_{\rm c}$	0.02	-0.04	0.02	0.07	0.08	1.00

Table 14: The reduced correlation matrix for the electroweak parameters from the 13-parameter fit.

The result of the full fit to the LEP/SLC results including the off-peak asymmetries and the b semileptonic branching ratio can be found in the appendix. It should be noted that the result on BR($\rm b \to \ell$) and the other non-electroweak parameters is independent of the treatment of the off-peak asymmetries and the SLD data.

5 The Hadronic Charge Asymmetry $\langle Q_{\rm FB} \rangle$

Updates from last year:
L3 has a new preliminary result based on 1991-1994 data.

The LEP experiments ALEPH [44–46], DELPHI [47,48], L3 [49] and OPAL [50,51] have provided measurements of the hadronic charge asymmetry based on the mean difference in jet charges measured in the forward and backward event hemispheres, $\langle Q_{\rm FB} \rangle$. DELPHI has also provided a related measurement of the total charge asymmetry by making a charge assignment on an event-by-event basis and performing a likelihood fit [47]. The experimental values quoted for the average forward-backward charge difference, $\langle Q_{\rm FB} \rangle$, cannot be directly compared as some of them include detector dependent effects such as acceptances and efficiencies. Therefore the effective electroweak mixing angle, $\sin^2\theta^{\rm lept}_{\rm eff}$, as defined in Section 7.3, is used as a means of combining the experimental results summarised in Table 15.

Experiment		$\sin^2\theta^{\rm lept}_{\rm eff}$
ALEPH	90-94, final	$0.2322 \pm 0.0008 \pm 0.0011$
DELPHI	91-94, prel.	$0.2311 \pm 0.0010 \pm 0.0014$
L3	91-94, prel.	$0.2336 \pm 0.0013 \pm 0.0014$
OPAL	91-94, prel.	$0.2326 \pm 0.0012 \pm 0.0013$
Average		0.2322 ± 0.0010

Table 15: Summary of the determination of $\sin^2\theta^{\rm lept}_{\rm eff}$ from inclusive hadronic charge asymmetries at LEP. For each experiment, the first error is statistical and the second systematic. The latter is dominated by fragmentation and decay modelling uncertainties.

The dominant source of systematic error arises from the modelling of the charge flow in the fragmentation process for each flavour. All experiments measure the required charge properties for $\mathrm{Z} \to \mathrm{b\overline{b}}$ events from the data. ALEPH also determines the charm charge properties from the data. The fragmentation model implemented in the JETSET Monte-Carlo program [52] is used by all experiments as reference; the one of the HERWIG Monte-Carlo program [53] is used for comparison. The JETSET fragmentation parameters are varied to estimate the systematic errors. The central values chosen by the experiments for these parameters are, however, not the same. The degree of correlation between the fragmentation uncertainties for the different experiments requires further investigation. The smaller of the two fragmentation errors in any pair of results is treated as common to both. The present average of $\sin^2\theta^{\rm lept}_{\rm eff}$ from $\langle Q_{\rm FB} \rangle$ and its associated error are not very sensitive to the treatment of common uncertainties. The ambiguities due to QCD corrections may cause changes in the derived value of $\sin^2\theta^{\rm lept}_{\rm eff}$. These are, however, well below the fragmentation uncertainties and experimental errors. The effect of fully correlating the estimated systematic uncertainties from this source between the experiments has a negligible effect upon the average and its error.

There is also some correlation between these results and those for $A^{\rm b\bar{b}}_{\rm FB}$ using jet charges. The dominant source of correlation is again through uncertainties in the fragmentation and decay models used. The typical correlation between the derived values of $\sin^2\theta^{\rm lept}_{\rm eff}$ between the $\langle Q_{\rm FB} \rangle$ and the $A^{\rm b\bar{b}}_{\rm FB}$ jet charge measurement has been estimated to be between 20% and 25%. This leads to only a small change in the relative weights for the $A^{\rm b\bar{b}}_{\rm FB}$ and $\langle Q_{\rm FB} \rangle$ results when averaging their $\sin^2\theta^{\rm lept}_{\rm eff}$ values (Section 7.3). Furthermore, the jet charge method contributes at most half of the weight of the $A^{\rm b\bar{b}}_{\rm FB}$ measurement. Thus, the correlation between $\langle Q_{\rm FB} \rangle$ and $A^{\rm b\bar{b}}_{\rm FB}$ from jet charge will have little impact on the overall Standard Model fit, and is neglected at present.

6 Measurement of the W mass at LEP

Updates from last year:
This is a new section.

In 1996 the energy of LEP was increased in two steps to 161 GeV and 172 GeV, thus allowing the production of pairs of W bosons at LEP. The data recorded at 161 GeV, which is just above the pair production threshold, can be used to determine the W mass by comparing the measured cross-section with the predicted cross-section behaviour. At higher energies, the mass can be determined by directly reconstructing the decay products of the W boson. Thus, in 1996 the LEP collaborations were able to determine the W mass using two complementary methods.

In the first run, at 161 GeV, each experiment accumulated a total luminosity of approximately 10 pb^{-1}. The final W pair cross-sections[6] determined by the 4 experiments [55–58] are shown in Table 16. Because of the low statistics (each experiment recorded only about 30 W pair events), the errors have been determined using Poisson statistics. To ease the determination of the average LEP cross-section, the experiments have also provided a symmetrized statistical error based on the number of expected events, given the world average W mass of 80.36 GeV [59]. This error is also shown in the table. The LEP average cross-section is

$$\sigma_{\mathrm{W^+W^-}} = 3.69 \pm 0.45 \text{ pb}, \tag{12}$$

where the smallest quoted systematic error (0.14) has been taken as 100% correlated between experiments. The χ^2 per degree of freedom is 1.3/3. The LEP centre-of-mass energy averaged over the 4 experiments has been determined to be 161.33 ± 0.05 [60]. Using the Gentle [61] program, the predicted cross-section as a function of the W mass can be calculated. This is shown in Fig 2. From this, the W mass is determined to be:

$$m_{\mathrm{W}} = 80.40^{+0.22}_{-0.21} \pm 0.03 \text{ GeV}, \tag{13}$$

where the first error is experimental, and the second error is due to the LEP energy calibration. Approximately 70 MeV of the experimental error is due to common systematics.

Experiment	$\sigma_{\mathrm{W^+W^-}}$ (pb)	Symmetrized stat. error
ALEPH	$4.23 \pm 0.73 \pm 0.19$	0.71
DELPHI	$3.67^{+0.97}_{-0.85} \pm 0.19$	0.91
L3	$2.89^{+0.81}_{-0.70} \pm 0.14$	0.92
OPAL	$3.62^{+0.93}_{-0.82} \pm 0.16$	0.88
LEP	3.69 ± 0.45	

Table 16: The $\mathrm{W^+W^-}$ cross-sections measured at 161 GeV. These results are all final.

Each experiment also accumulated 10 pb^{-1} at the higher energy of 172 GeV. The cross-section at 172 GeV is more than a factor 3 higher than at 161 GeV, so that each experiment recorded approximately 100 W pair events at this energy. To determine the W mass, the experiments fit the reconstructed invariant mass distributions [62–65]. The results are shown in Table 17. The systematic errors quoted include experimental sources, the LEP energy uncertainty of 30 MeV, and in the case of the $\mathrm{q\bar{q}q\bar{q}}$ channel 100 MeV from potential effects of colour reconnection [54]. In the combination, these

[6] The cross-section measurements reported here have been corrected by the experiments to correspond to the CC03 [54] set of diagrams.

Experiment	m_{W} (GeV)	
	$\mathrm{q\bar{q}}\ell\nu$	$\mathrm{q\bar{q}q\bar{q}}$
ALEPH (prel.)	$80.38 \pm 0.43 \pm 0.12$	$81.30 \pm 0.47 \pm 0.10$
DELPHI (prel.)	$80.51 \pm 0.57 \pm 0.06$	$79.90 \pm 0.59 \pm 0.12$
L3 (final)	$80.42 \pm 0.54 \pm 0.08$	$80.91 \pm 0.42 \pm 0.13$
OPAL (prel.)	$80.53 \pm 0.41 \pm 0.10$	$80.08 \pm 0.44 \pm 0.15$
LEP	80.46 ± 0.24	80.62 ± 0.26

Table 17: The measurements of m_{W} at 172 GeVin the $\mathrm{q\bar{q}}\ell\nu$ and $\mathrm{q\bar{q}q\bar{q}}$ channels. The χ^2/d.o.f. for the two combinations is 0.1/3 and 5.4/3.

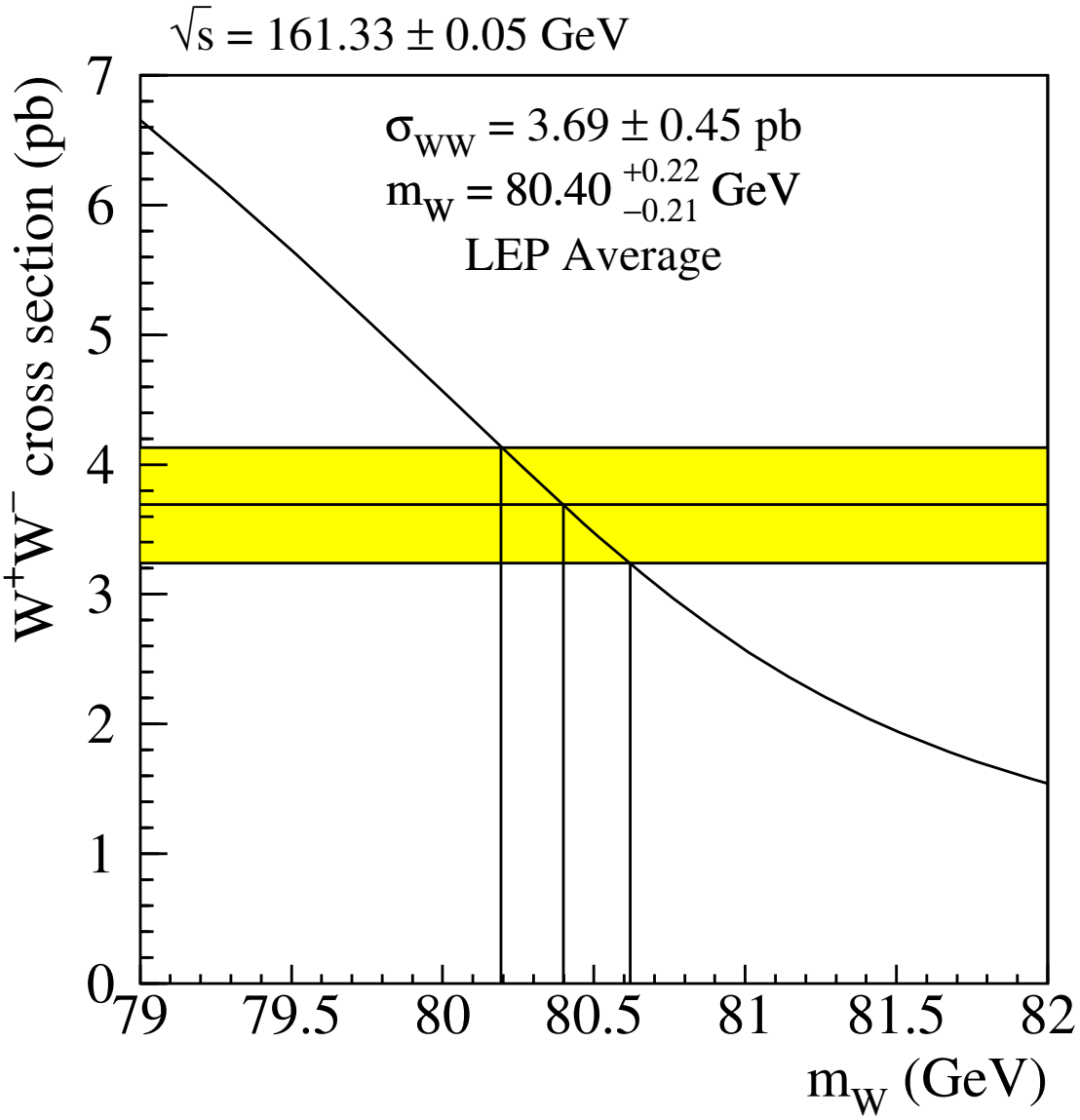

Figure 2: The cross-section of the process $\mathrm{e^+e^-} \to \mathrm{W^+W^-}$ as a function of the W mass. The horizontal band shows the cross-section measurement with its error. The curve shows the Standard Model prediction.

last two systematic errors have been treated as 100% correlated. At the current level of statistics, the mass determined from semi-leptonic decays and that from hadronic decays are consistent, and are combined to obtain:

$$m_{\mathrm{W}} = 80.53 \pm 0.17 \pm 0.05 \text{ GeV}. \tag{14}$$

Combining this last result, with that of the 161 GeV data yields

$$m_{\mathrm{W}} = 80.48 \pm 0.13 \pm 0.04 \text{ GeV} \tag{15}$$

as the current LEP average W mass.

In addition, the LEP experiments have determined the W pair cross-section at 172 GeV, and have used the data at 161 and 172 GeV to determine the W decay branching ratios. These results are summarized in Figure 3 and Tables 18 and 19.

Experiment	$\sigma_{\mathrm{W^+W^-}}$ (pb)
ALEPH (final)	$11.71 \pm 1.23 \pm 0.28$
DELPHI (prel.)	$11.58^{+1.44}_{-1.35} \pm 0.32$
L3 (final)	$12.27^{+1.41}_{-1.32} \pm 0.23$
OPAL (prel.)	$12.3 \pm 1.3 \pm 0.3$
LEP	12.0 ± 0.7

Table 18: The measurements of the W pair cross-sections at 172 GeV.

Experiment	Br(W$\to$eν)	Br(W$\to \mu\nu$)	Br(W$\to \tau\nu$)	Br(W$\to$hadrons)
ALEPH (final)	9.7 ± 2.2	11.2 ± 2.2	11.3 ± 2.9	67.7 ± 3.2
DELPHI (prel.)	10.2 ± 3.8	10.7 ± 3.2	13.4 ± 5.0	66.0 ± 3.7
L3 (final)	16.5 ± 3.7	8.4 ± 2.8	10.9 ± 4.2	64.2 ± 3.7
OPAL (prel.)	9.8 ± 2.1	7.3 ± 1.8	14.0 ± 2.9	69.8 ± 3.2
LEP	10.8 ± 1.3	9.2 ± 1.1	12.7 ± 1.7	67.2 ± 1.7

Table 19: The measurements of the W decay branching ratios in percent. The hadronic branching ratio is determined assuming lepton universality. There are large correlations between the individual leptonic branching ratios, which have been taken into account in determining the hadronic branching ratio.

7 Interpretation of Results

Updates from last year:
The results of the Standard Model fit with the Higgs mass as a free parameter are presented. A new fit is performed, where all data except the direct measurements of m_{W} and m_{t} are included.

7.1 The Coupling Parameters $\mathcal{A}_{\mathrm{f}}$

The coupling parameters $\mathcal{A}_{\mathrm{f}}$ are defined in terms of the effective vector and axial-vector neutral current couplings of fermions (Equation (3)). The LEP measurements of the forward-backward asymmetries

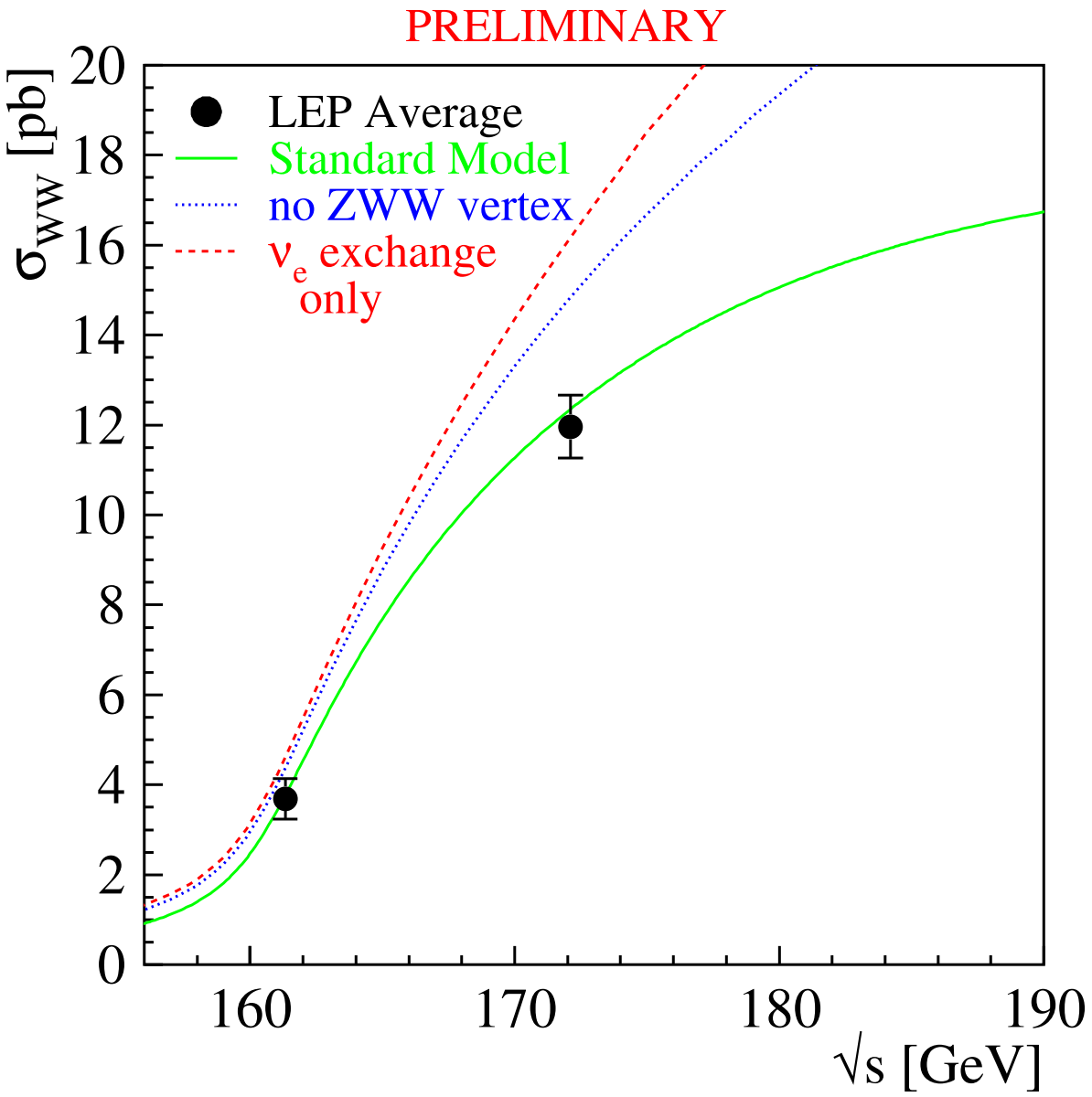

Figure 3: The W pair cross-section as a function of the center of mass energy. The data points are the LEP averages. Also shown is the Standard Model prediction (solid line), and for comparison the cross-section if the ZWW coupling did not exist (dotted line), or if only the t-channel ν_e exchange diagram existed (dashed line).

of charged leptons (Section 2) and b and c quarks (Section 4) determine the products $A_{\rm FB}^{0,{\rm f}} = \frac{3}{4}\mathcal{A}_{\rm e}\mathcal{A}_{\rm f}$ (Equation (2)). The LEP measurements of the τ polarisation (Section 3), $\mathcal{P}_\tau(\cos\theta)$, determine $\mathcal{A}_\tau$ and $\mathcal{A}_{\rm e}$ separately (Equation (5)). The SLD collaboration measures the left-right asymmetry, $A_{\rm LR}$ [66], which determines the same quantity, $\mathcal{A}_{\rm e}$, as the τ polarisation, with minimal model dependence. Both measurements have small systematic errors. Table 20 shows the results for the leptonic coupling parameter $\mathcal{A}_\ell$ and their combination assuming lepton universality. The LEP lepton asymmetries and tau polarization measurements disagree at the 2 sigma level (3% probability). The addition of the SLD $A_{\rm LR}$ measurement does not significantly change the probability of χ^2. It should be noted that all of these results are statistics dominated.

	$\mathcal{A}_\ell$	Cumulative Average	χ^2/d.o.f.
$A_{\rm FB}^{0,\ell}$	0.1510 ± 0.0044		
$\mathcal{P}_\tau(\cos\theta)$	0.1406 ± 0.0048	0.1461 ± 0.0033	2.5/1
$A_{\rm LR}$ (SLD)	0.1547 ± 0.0032	0.1505 ± 0.0023	6.0/2

Table 20: Comparison of the determinations of the leptonic coupling parameter $\mathcal{A}_\ell$ assuming lepton universality. The second column lists the $\mathcal{A}_\ell$ values derived from the quantities listed in the first column. The third column contains the cumulative averages of these $\mathcal{A}_\ell$ results. The averages are derived assuming no correlations between the measurements. The χ^2 per degree of freedom for the cumulative averages is given in the last column.

Using the measurements of $\mathcal{A}_\ell$ one can extract $\mathcal{A}_{\rm b}$ and $\mathcal{A}_{\rm c}$ from the LEP measurements of the b and c quark asymmetries. The SLD measurements of the left-right forward-backward asymmetries for b and c quarks [66] are direct determinations of $\mathcal{A}_{\rm b}$ and $\mathcal{A}_{\rm c}$. Table 21 shows the results on the quark coupling parameters $\mathcal{A}_{\rm b}$ and $\mathcal{A}_{\rm c}$ derived from LEP or SLD measurements separately (Equations 10 and 11) and from the combination of LEP and SLD measurements (Equation 11). The LEP only extractions of $\mathcal{A}_{\rm b}$ and $\mathcal{A}_{\rm c}$ are in excellent agreement with the SLD measurements, and in reasonable agreement with the Standard Model predictions (0.935 and 0.668, respectively; see Table 24). However, the combination of LEP+SLD of $\mathcal{A}_{\rm b}$ is about 2.5 sigma below the Standard Model. This is due to three independent measurements: the LEP measurement of $A_{\rm FB}^{0,\rm b}$ is low compared to the Standard Model; the SLD measurement of $\mathcal{A}_{\rm b}$ is also slightly lower; and the SLD measurement of $A_{\rm LR}$ is high compared to the Standard Model.

	LEP ($\mathcal{A}_\ell = 0.1461 \pm 0.0033$)	SLD	LEP+SLD ($\mathcal{A}_\ell = 0.1505 \pm 0.0023$)
$\mathcal{A}_{\rm b}$	0.897 ± 0.030	0.900 ± 0.050	0.877 ± 0.023
$\mathcal{A}_{\rm c}$	0.674 ± 0.046	0.650 ± 0.058	0.653 ± 0.037

Table 21: Determinations of the quark coupling parameters $\mathcal{A}_{\rm b}$ and $\mathcal{A}_{\rm c}$ from LEP data alone (using the LEP average for $\mathcal{A}_\ell$), from SLD data alone, and from LEP+SLD data (using the LEP+SLD average for $\mathcal{A}_\ell$) assuming lepton universality.

7.2 The Effective Vector and Axial-Vector Coupling Constants

The partial widths of the Z into leptons and the lepton forward-backward asymmetries (Section 2), the τ polarisation and the τ polarisation asymmetry (Section 3) can be combined to determine the effective vector and axial-vector couplings for e, μ and τ. The asymmetries (Equations (2) and (5)) determine the ratio $g_{V\ell}/g_{A\ell}$ (Equation (3)), while the sum of the squares of the couplings is derived from the leptonic partial widths:

$$\Gamma_{\ell\ell} = \frac{G_{\rm F} m_{\rm Z}^3}{6\pi\sqrt{2}}(g_{V\ell}^2 + g_{A\ell}^2)(1 + \delta_\ell^{QED}), \tag{16}$$

where $\delta_\ell^{QED} = 3q_\ell^2\alpha(m_{\rm Z}^2)/(4\pi)$ accounts for final state photonic corrections. Corrections due to lepton masses, neglected in Equation 16, are taken into account for the results presented below.

The averaged results for the effective lepton couplings are given in Table 22. Figure 4 shows the 68% probability contours in the $g_{A\ell}$-$g_{V\ell}$ plane. The signs of $g_{A\ell}$ and $g_{V\ell}$ are based on the convention

$g_{Ae} < 0$. With this convention the signs of the couplings of all charged leptons follow from LEP data alone. For comparison, the $g_{V\ell}$-$g_{A\ell}$ relation following from the measurement of A_{LR} from SLD [66] is indicated as a band in the $g_{A\ell}$-$g_{V\ell}$-plane of Figure 4. It is consistent with the LEP data. The information on the leptonic couplings from LEP can therefore be combined with the A_{LR} measurement of SLD. The results for this combination are given in the right column of Table 22. The measured ratios of the e, μ and τ couplings provide a test of lepton universality and are also given in Table 22.

	Without Lepton Universality:	
	LEP	LEP+SLD
g_{Ve}	-0.0367 ± 0.0015	-0.03844 ± 0.00071
$g_{V\mu}$	-0.0374 ± 0.0036	-0.0358 ± 0.0032
$g_{V\tau}$	-0.0367 ± 0.0015	-0.0365 ± 0.0015
g_{Ae}	-0.50123 ± 0.00044	-0.50111 ± 0.00043
$g_{A\mu}$	-0.50087 ± 0.00066	-0.50098 ± 0.00065
$g_{A\tau}$	-0.50102 ± 0.00074	-0.50103 ± 0.00074
	Ratios of couplings:	
	LEP	LEP+SLD
$g_{V\mu}/g_{Ve}$	1.02 ± 0.12	0.932 ± 0.087
$g_{V\tau}/g_{Ve}$	0.998 ± 0.060	0.949 ± 0.044
$g_{A\mu}/g_{Ae}$	0.9993 ± 0.0017	0.9997 ± 0.0016
$g_{A\tau}/g_{Ae}$	0.9996 ± 0.0018	0.9998 ± 0.0018
	With Lepton Universality:	
	LEP	LEP+SLD
$g_{V\ell}$	-0.03681 ± 0.00085	-0.03793 ± 0.00058
$g_{A\ell}$	-0.50112 ± 0.00032	-0.50103 ± 0.00031
g_ν	$+0.50125 \pm 0.00092$	$+0.50125 \pm 0.00092$

Table 22: Results for the effective vector and axial-vector couplings derived from the combined LEP data without and with the assumption of lepton universality. For the right column the SLD measurement of A_{LR} is also included.

The neutrino couplings to the Z can be derived from the measured value of its invisible width, Γ_{inv} (see Table 9), attributing it exclusively to the decay into three identical neutrino generations ($\Gamma_{inv} = 3\Gamma_{\nu\nu}$) and assuming $g_{A\nu} \equiv g_{V\nu} \equiv g_\nu$. The relative sign of g_ν is chosen to be in agreement with neutrino scattering data [67], resulting in $g_\nu = +0.50125 \pm 0.00092$.

7.3 The Effective Electroweak Mixing Angle $\sin^2\theta^{lept}_{eff}$

The asymmetry measurements from LEP can be combined into a single observable, the effective electroweak mixing angle, $\sin^2\theta^{lept}_{eff}$, defined as:

$$\sin^2\theta^{lept}_{eff} \equiv \frac{1}{4}(1 - g_{V\ell}/g_{A\ell}) , \tag{17}$$

without making any strong model-specific assumptions.

For a combined average of $\sin^2\theta^{lept}_{eff}$ from $A^{0,\ell}_{FB}$, $\mathcal{A}_\tau$ and $\mathcal{A}_e$ only the assumption of lepton universality, already inherent in the definition of $\sin^2\theta^{lept}_{eff}$, is needed. We can also include the hadronic forward-backward asymmetries if we assume the hadronic couplings to be given by the Standard Model. This is justified within the Standard Model as the hadronic asymmetries $A^{0,b}_{FB}$ and $A^{0,c}_{FB}$ have a reduced

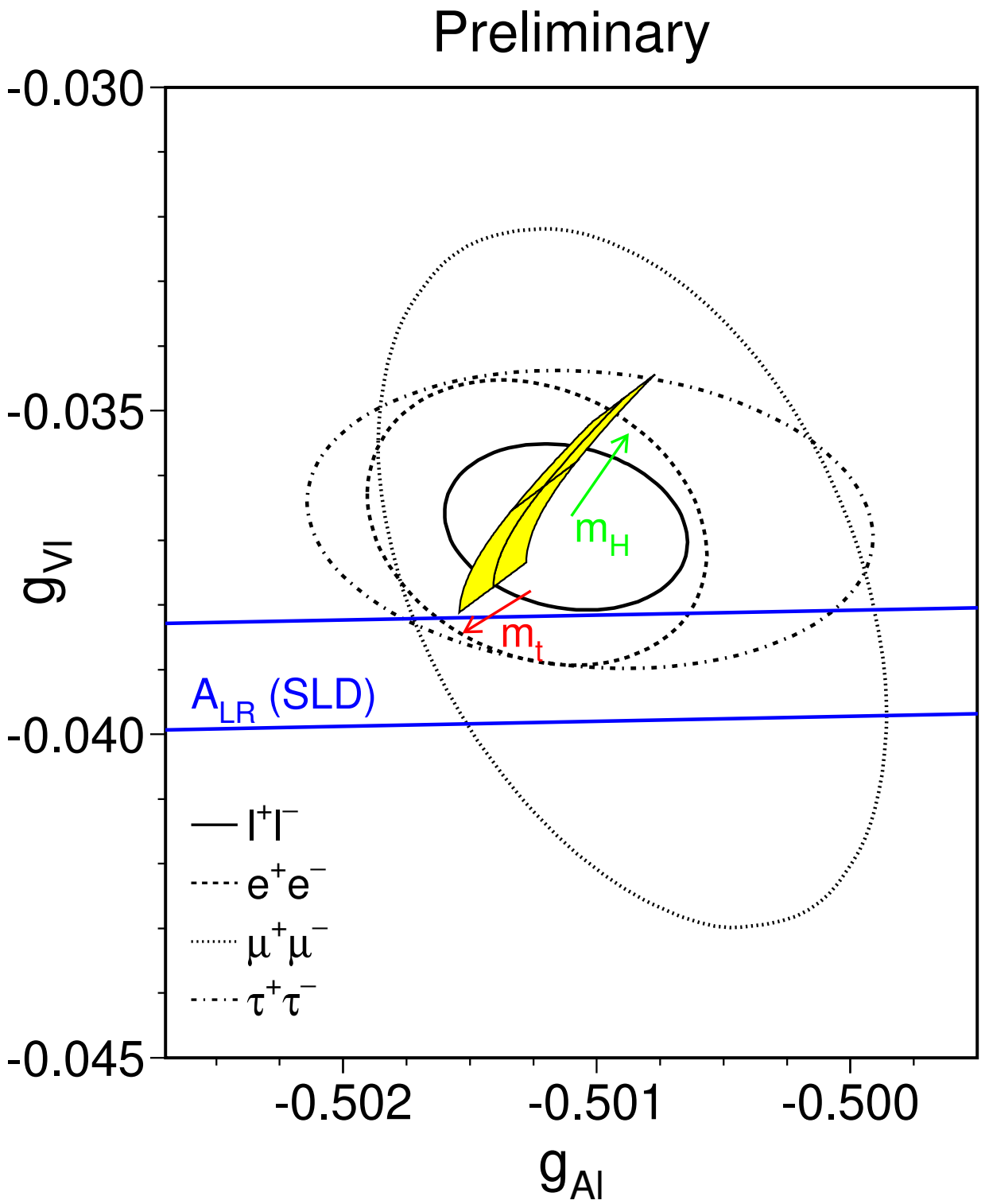

Figure 4: Contours of 68% probability in the $g_{V\ell}$-$g_{A\ell}$ plane from LEP measurements. The solid contour results from a fit assuming lepton universality. Also shown is the one standard deviation band resulting from the $A_{\rm LR}$ measurement of SLD. The shaded region corresponds to the Standard Model prediction for $m_{\rm t} = 175.6 \pm 5.5$ GeV and $m_{\rm H} = 300^{+700}_{-240}$ GeV. The arrows point in the direction of increasing values of $m_{\rm t}$ and $m_{\rm H}$.

sensitivity to weak corrections and to those corrections particular to the hadronic vertex. The results of these determinations of $\sin^2\theta^{\rm lept}_{\rm eff}$ and their combination are shown in Table 23. Also the measurement of the left-right asymmetry, $A_{\rm LR}$, from SLD [66] is given. Compared to the results presented in our previous note [1], the χ^2 of the average of all determinations has decreased by 0.3.

	$\sin^2\theta^{\rm lept}_{\rm eff}$	Average by Group of Observations	Cumulative Average	χ^2/d.o.f.
$A^{0,\ell}_{\rm FB}$	0.23102 ± 0.00056			
$\mathcal{A}_\tau$	0.23228 ± 0.00081			
$\mathcal{A}_{\rm e}$	0.23243 ± 0.00093	0.23162 ± 0.00041	0.23162 ± 0.00041	2.6/2
$A^{0,\rm b}_{\rm FB}$	0.23236 ± 0.00043			
$A^{0,\rm c}_{\rm FB}$	0.23140 ± 0.00111	0.23223 ± 0.00040	0.23194 ± 0.00029	4.3/4
$\langle Q_{\rm FB}\rangle$	0.2322 ± 0.0010	0.2322 ± 0.0010	0.23196 ± 0.00028	4.4/5
$A_{\rm LR}$ (SLD)	0.23055 ± 0.00041	0.23055 ± 0.00041	0.23152 ± 0.00023	12.5/6

Table 23: Comparison of several determinations of $\sin^2\theta^{\rm lept}_{\rm eff}$ from asymmetries. Averages are obtained as weighted averages assuming no correlations. The second column lists the $\sin^2\theta^{\rm lept}_{\rm eff}$ values derived from the quantities listed in the first column. The third column contains the averages of these numbers by groups of observations, where the groups are separated by the horizontal lines. The last column shows the cumulative averages. The χ^2 per degree of freedom for the cumulative averages is also given.

7.4 Number of Neutrino Species

An important aspect of our measurement concerns the information related to Z decays into invisible channels. Using the results of Tables 7 and 8, the ratio of the Z decay width into invisible particles and the leptonic decay width is determined:

$$\Gamma_{\rm inv}/\Gamma_{\ell\ell} \;=\; 5.960 \pm 0.022\,.$$

The Standard Model value for the ratio of the partial widths to neutrinos and charged leptons is:

$$(\Gamma_{\nu\nu}/\Gamma_{\ell\ell})_{\rm SM} \;=\; 1.991 \pm 0.001\,.$$

The central value is evaluated for $m_{\rm Z} = 91.1867$ GeV, $m_{\rm t} = 175.6$ GeV, $m_{\rm H} = 300$ GeV and the error quoted accounts for a variation of $m_{\rm t}$ in the range $m_{\rm t} = 175.6 \pm 5.5$ GeV and a variation of $m_{\rm H}$ in the range 60 GeV $\leq m_{\rm H} \leq$ 1000 GeV.

The number of light neutrino species is given by the ratio of the two expressions listed above:

$$N_\nu \;=\; 2.993 \pm 0.011\,.$$

Alternatively, one can assume 3 neutrino species, and extract the 95% CL upper limit on additional invisible decays of the Z. As is evident from the equations shown in section 2, a change in the width would affect not only the total width, but also the peak hadronic cross-section. To extract the

additional width, a term is added to the total width, and the fit (described in the next section) to the Standard Model is performed. This fit results in

$$\Delta\Gamma_{\rm inv} = -1.2 \pm 1.8 \text{ MeV}. \tag{18}$$

That the additional width is negative is simply that the measured total width is slightly lower than the Standard Model expectation. This is also seen in the number of neutrino families which is slightly lower than 3. If a conservative approach is taken to limit the result to only positive values of $\Delta\Gamma_{\rm inv}$, then the 95% CL upper limit on additional invisible decays of the Z is

$$\Delta\Gamma_{\rm inv} < 2.8 \text{ MeV}. \tag{19}$$

7.5 Constraints on the Standard Model

The precise electroweak measurements performed at LEP can be used to check the validity of the Standard Model and, within its framework, to infer valuable information about its fundamental parameters. The accuracy of the measurements makes them sensitive to the top-quark mass, $m_{\rm t}$, and to the mass of the Higgs boson, $m_{\rm H}$, through loop corrections. While the leading $m_{\rm t}$ dependence is quadratic, the leading $m_{\rm H}$ dependece is logarithmic. Therefore, the inferred constraints on $m_{\rm H}$ are not very strong.

The LEP measurements used are summarised in Table 24a together with the Standard Model predictions. Also shown are the results from the SLD collaboration [66] as well as measurements of $m_{\rm W}$ from UA2 [76], CDF [77, 78], and DØ [79][7], measurements of the neutrino neutral to charged current ratios from CDHS [70], CHARM [71] and CCFR [72], and the measurement of the top quark mass [73–75] by CDF and DØ. In addition, the determination of the electromagnetic coupling constant, $\alpha(m_{\rm Z}^2)$, which is used in the fits, is shown. An additional input parameter, not shown in the table, is the Fermi constant, G_F, determined from the muon lifetime, $G_F = 1.16639 \times 10^{-5}\text{GeV}^{-2}$ [80].

Detailed studies of the theoretical uncertainties in the Standard Model predictions due to missing higher-order electroweak corrections and their interplay with QCD corrections are carried out in the working group on 'Precision calculations for the Z resonance' [81]. Theoretical uncertainties are evaluated by comparing different but, within our present knowledge, equivalent treatments of aspects such as resummation techniques, momentum transfer scales for vertex corrections and factorisation schemes. The impact of these intrinsic theoretical uncertainties on $m_{\rm t}$ and $\alpha_s(m_{\rm Z}^2)$ has been estimated by repeating the Standard Model fits in this Section using several combinations of options which were implemented in the electroweak libraries used [82] for the study performed in Reference 81. As a result the maximal variations of the central values of the fitted parameters correspond to an additional theoretical error of less than 1 GeV on $m_{\rm t}$, less than 0.001 on $\alpha_s(m_{\rm Z}^2)$ and 0.1 on $\log(m_{\rm H})$. Although the theoretical error on $\log(m_{\rm H})$ is still smaller than the experimental error, it is relatively more important than the theoretical error on $m_{\rm t}$ or $\alpha_s(m_{\rm Z}^2)$. The theoretical error on $\alpha_s(m_{\rm Z}^2)$ covers missing higher-order electroweak corrections and uncertainties in the interplay of electroweak and QCD corrections. The effect of missing higher-order QCD corrections on $\alpha_s(m_{\rm Z}^2)$ has been estimated to be about 0.002 [83]. A discussion of theoretical uncertainties in the determination of α_s can be found in References 81 and 83. Recently, new calculations of higher-order corrections have become available [84]. However, as some of these calculations are not yet complete, and are not yet fully incorporated in the electroweak libraries, the results quoted here are still based on Ref. [82]. In addition, all theoretical errors discussed in this paragraph have been neglected for the results presented in Table 25.

[7] See Reference 69 for a combination of these $m_{\rm W}$ measurements.

		Measurement with Total Error	Systematic Error	Standard Model	Pull
	$\alpha(m_{\rm Z}^2)^{-1}$ [68]	128.896 ± 0.090	0.083	128.898	-0.0
a)	LEP				
	line-shape and				
	lepton asymmetries:				
	$m_{\rm Z}$ [GeV]	91.1867 ± 0.0020	[(a)]0.0015	91.1866	0.0
	$\Gamma_{\rm Z}$ [GeV]	2.4948 ± 0.0025	[(a)]0.0015	2.4966	-0.7
	$\sigma_{\rm h}^0$ [nb]	41.486 ± 0.053	0.052	41.467	0.4
	R_ℓ	20.775 ± 0.027	0.024	20.756	0.7
	$A_{\rm FB}^{0,\,\ell}$	0.0171 ± 0.0010	0.0007	0.0162	0.9
	+ correlation matrix Table 8				
	τ polarisation:				
	$\mathcal{A}_\tau$	0.1411 ± 0.0064	0.0040	0.1470	-0.9
	$\mathcal{A}_{\rm e}$	0.1399 ± 0.0073	0.0020	0.1470	-1.0
	b and c quark results:				
	$R_{\rm b}^{0\,(b)}$	0.2174 ± 0.0009	0.0007	0.2158	1.8
	$R_{\rm c}^{0\,(b)}$	0.1727 ± 0.0050	0.0038	0.1723	-0.1
	$A_{\rm FB}^{0,\,{\rm b}\,(b)}$	0.0983 ± 0.0024	0.0010	0.1031	-2.0
	$A_{\rm FB}^{0,\,{\rm c}\,(b)}$	0.0739 ± 0.0048	0.0025	0.0736	0.0
	+ correlation matrix Table 13				
	$\rm q\overline{q}$ charge asymmetry:				
	$\sin^2\theta_{\rm eff}^{\rm lept}$ ($\langle Q_{\rm FB}\rangle$)	0.2322 ± 0.0010	0.0008	0.23152	0.7
	$m_{\rm W}$ [GeV]	80.48 ± 0.14	0.05	80.375	0.8
b)	SLD [66]				
	$\sin^2\theta_{\rm eff}^{\rm lept}$ ($A_{\rm LR}$)	0.23055 ± 0.00041	0.00014	0.23152	-2.4
	$R_{\rm b}^{0\,(b)}$	0.2124 ± 0.0029	0.0017	0.2158	-1.1
	$R_{\rm c}^{0\,(b)}$	0.1810 ± 0.0145	0.0079	0.1723	0.6
	$\mathcal{A}_{\rm b}$	0.900 ± 0.050	0.031	0.935	-0.7
	$\mathcal{A}_{\rm c}$	0.650 ± 0.058	0.029	0.668	-0.3
c)	$\rm p\overline{p}$ and νN				
	$m_{\rm W}$ [GeV] ($\rm p\overline{p}$ [69])	80.41 ± 0.09	0.07	80.375	0.4
	$1 - m_{\rm W}^2/m_{\rm Z}^2$ (νN [70–72])	0.2254 ± 0.0037	0.0023	0.2231	0.6
	$m_{\rm t}$ [GeV] ($\rm p\overline{p}$ [73–75])	175.6 ± 5.5	4.2	173.1	0.4

Table 24: Summary of measurements included in the combined analysis of Standard Model parameters. Section a) summarises LEP averages, Section b) SLD results ($\sin^2\theta_{\rm eff}^{\rm lept}$ includes $A_{\rm LR}$ and the polarized lepton asymmetries) and Section c) electroweak measurements from $\rm p\overline{p}$ colliders and νN scattering. The total errors in column 2 include the systematic errors listed in column 3. The determination of the systematic part of each error is approximate. The Standard Model results in column 4 and the pulls (difference between measurement and fit in units of the total measurement error) in column 5 are derived from the Standard Model fit including all data (Table 25, column 3) with the Higgs mass treated as a free parameter.

[(a)] The systematic errors on $m_{\rm Z}$ and $\Gamma_{\rm Z}$ contain the errors arising from the uncertainties in the LEP energy only.

[(b)] For fits which combine LEP and SLD heavy flavour measurements we use as input the heavy flavour results given in Equation (11) and their correlation matrix in Table 14 in Section 4 of this note.

At present the impact of theoretical uncertainties on the determination of $m_{\rm t}$ from precise electroweak measurements is small compared to the error due to the uncertainty in the value of $\alpha(m_{\rm Z}^2)$. The uncertainty in $\alpha(m_{\rm Z}^2)$ arises from the contribution of light quarks to the photon vacuum polarisation. Recently there have been several reevaluations of $\alpha(m_{\rm Z}^2)$ [68, 85–88]. For the results presented in this Section, a value of $\alpha(m_{\rm Z}^2) = 1/(128.896 \pm 0.090)$ [68] is used. This uncertainty causes an error of 0.00023 on the Standard Model prediction of $\sin^2\theta_{\rm eff}^{\rm lept}$, an error of 1 GeV on $m_{\rm t}$, and and 0.2 on $\log(m_{\rm H})$, which are included in the results listed in Table 25. The effect on the Standard Model prediction for $\Gamma_{\ell\ell}$ is negligible. The $\alpha_s(m_{\rm Z}^2)$ values for the Standard Model fits presented in this Section are stable against a variation of $\alpha(m_{\rm Z}^2)$ in the interval quoted.

Figure 6 shows a comparison of the leptonic partial width from LEP (Table 9) and the effective electroweak mixing angle from asymmetries measured at LEP and SLD (Table 23), with the Standard Model. Good agreement with the Standard Model prediction is observed. The star shows the prediction if, among the electroweak radiative corrections only the photon vacuum polarisation is included, showing evidence that LEP/SLD data are sensitive to genuine electroweak corrections. Note that the error due to the uncertainty on $\alpha(m_{\rm Z}^2)$ (shown as the length of the arrow attached to the star) is as large as the experimental error on $\sin^2\theta_{\rm eff}^{\rm lept}$ from LEP and SLD.

The value of $\alpha_s(m_{\rm Z}^2)$ derived from an analysis of electroweak precision tests within the Standard Model framework depends essentially on R_ℓ, $\Gamma_{\rm Z}$ and $\sigma_{\rm h}^0$. The result is in very good agreement with the world average ($\alpha_s(m_{\rm Z}^2) = 0.118 \pm 0.003$ [80]) and is of similar precision. The strong coupling constant can also be determined from the parameter R_ℓ alone. For $m_{\rm Z} = 91.1867$ GeV, and imposing $m_{\rm t} = 175.6 \pm 5.5$ GeV as a constraint, $\alpha_s = 0.124 \pm 0.004 \pm 0.002$ is obtained, where the second error accounts for the variation of the result when varying $m_{\rm H}$ in the range 60 GeV $\leq m_{\rm H} \leq$ 1000 GeV.

In Figure 7 the fitted result for $R_{\rm b}$ with $R_{\rm c}$ fixed to its Standard Model value is plotted versus $\sin^2\theta_{\rm eff}^{\rm lept}$. If one assumes the Standard Model dependence of the partial widths on $\sin^2\theta_{\rm eff}^{\rm lept}$ for the light quarks and the c quark, and takes $\alpha_s(m_{\rm Z}^2) = 0.118 \pm 0.003$, R_ℓ imposes a constraint on the two variables. A good agreement is seen for these 3 experimentally independent measurements, showing the consistency of the LEP data.

To constrain $m_{\rm H}$, we first perform a fit to the LEP data alone (including the LEP-II $m_{\rm W}$ determination) leaving the top quark mass and the Higgs mass as free parameters. The result is shown in Table 25, column 2. This fit shows that the LEP data prefer a light top quark and a light Higgs, albeit with very large errors. The strongly asymmetric errors on $m_{\rm H}$ are due to the fact that to first order, the radiative corrections in the Standard Model are proportional to $\log(m_{\rm H})$. The correlation between the top quark mass and the Higgs mass is 0.76 (see Figure 9). It should be noted that the correlation would be even larger if the $R_{\rm b}$ measurement is not used, as $R_{\rm b}$ is insensitive to $m_{\rm H}$.

The data can also be used within the Standard Model to determine the top quark and W masses indirectly, and compare them to the direct measurements performed at the Tevatron and LEP. For this fit, we use all the results in Table 24, except the LEP-II and Tevatron $m_{\rm W}$ and $m_{\rm t}$ results. The results of the fit are shown in column 3 of Table 25. The indirect measurements of $m_{\rm W}$ and $m_{\rm t}$ from this data sample are shown in Figure 8, compared to the direct measurements. Also shown is the Standard Model predictions for Higgs masses between 60 and 1000 GeV. As can be seen in both the table and the figure, the indirect measurements prefer low $m_{\rm t}$ and low $m_{\rm H}$.

The best constraints on $m_{\rm H}$ are obtained when all data, especially the direct measurements of $m_{\rm t}$, are used in the fit. The results of this fit are shown in the last column of Table 25 and in Figure 9. In Figures 10 and 11 the sensitivity of the LEP measurements to the Higgs mass is shown. As can be seen, the most sensitive measurements are the asymmetries. A reduced uncertainty for the value of

$\alpha(m_{\rm Z}^2)$ would therefore result in an improved constraint on $m_{\rm H}$, as shown in Figure 6.

	LEP (including LEP-II $m_{\rm W}$)	all data except $m_{\rm t}$ and $m_{\rm W}$	all data
$m_{\rm t}$ [GeV]	158^{+14}_{-11}	157^{+10}_{-9}	173.1 ± 5.4
$m_{\rm H}$ [GeV]	83^{+168}_{-49}	41^{+64}_{-21}	115^{+116}_{-66}
$\log(m_{\rm H})$	$1.92^{+0.48}_{-0.39}$	$1.62^{+0.41}_{-0.31}$	$2.06^{+0.30}_{-0.37}$
$\alpha_s(m_{\rm Z}^2)$	0.121 ± 0.003	0.120 ± 0.003	0.120 ± 0.003
χ^2/d.o.f.	8/9	14/12	17/15
$\sin^2\theta^{\rm lept}_{\rm eff}$	0.23188 ± 0.00026	0.23153 ± 0.00023	0.23152 ± 0.00022
$1 - m_{\rm W}^2/m_{\rm Z}^2$	0.2246 ± 0.0008	0.2240 ± 0.0008	0.2231 ± 0.0006
$m_{\rm W}$ (GeV)	80.298 ± 0.043	80.329 ± 0.041	80.375 ± 0.030

Table 25: Results of the fits to LEP data alone, to all data except the direct determinations of $m_{\rm t}$ and $m_{\rm W}$ (Tevatron and LEP-II) and to all data including the top quark mass determination. As the sensitivity to $m_{\rm H}$ is logarithmic, both $m_{\rm H}$ as well as $\log(m_{\rm H})$ are quoted. The bottom part of the table lists derived results for $\sin^2\theta^{\rm lept}_{\rm eff}$, $1 - m_{\rm W}^2/m_{\rm Z}^2$ and $m_{\rm W}$. See text for a discussion of theoretical errors not included in the errors above.

In Figure 12 the observed value of $\Delta\chi^2 \equiv \chi^2 - \chi^2_{min}$ as a function of $m_{\rm H}$ is plotted for the fit including all data. The shaded band shows the additional error due to the missing higher order corrections. Taking this error into account yields the one-sided 95% confidence level upper limit on $m_{\rm H}$ of 420 GeV. The lower limit on $m_{\rm H}$ of approximately 70 GeV obtained from direct searches [89] has not been used in this limit determination.

8 Prospects for the Future

The LEP energy has now been increased; the Z phase of LEP has come to an end. However, the analyses of the data are not yet finished. The major improvements which should happen in the near future will be:

- completion of the lineshape analysis, including final LEP energy calibrations. The biggest improvement should be in the measurement of $\Gamma_{\rm Z}$;
- improved measurements of $R_{\rm b}$ using new techniques;
- completion of the τ polarisation measurements, especially of the statistics dominated measurement of $\mathcal{A}_{\rm e}$;
- the errors on the measurements from SLD ($A_{\rm LR}$, $R_{\rm b}$, $\mathcal{A}_{\rm b}$ and $\mathcal{A}_{\rm c}$) should decrease by a factor of approximately 1.5.

In addition, the measurements of $m_{\rm W}$ at both the TEVATRON and LEP are beginning to match the error obtained via the radiative corrections of the Z data, and providing a further important test of the Standard Model.

9 Conclusions

The combination of the many precise electroweak results yields stringent constraints on the Standard Model. All LEP measurements agree well with the predictions. Including all measurements, the data show some sensitivity to the Higgs mass.

The LEP experiments wish to stress that this report reflects a preliminary status at the time of the 1997 summer conferences. A definitive statement on these results has to wait for publication by each collaboration.

Acknowledgments

We would like to thank the SL Division of CERN for the efficient operation of the LEP accelerator, the precise information on the absolute energy scale and their close cooperation with the four experiments. We would also like to thank members of the CDF, DØ and SLD Collaborations for making results available to us in advance of the conferences and for useful discussions concerning their combination.

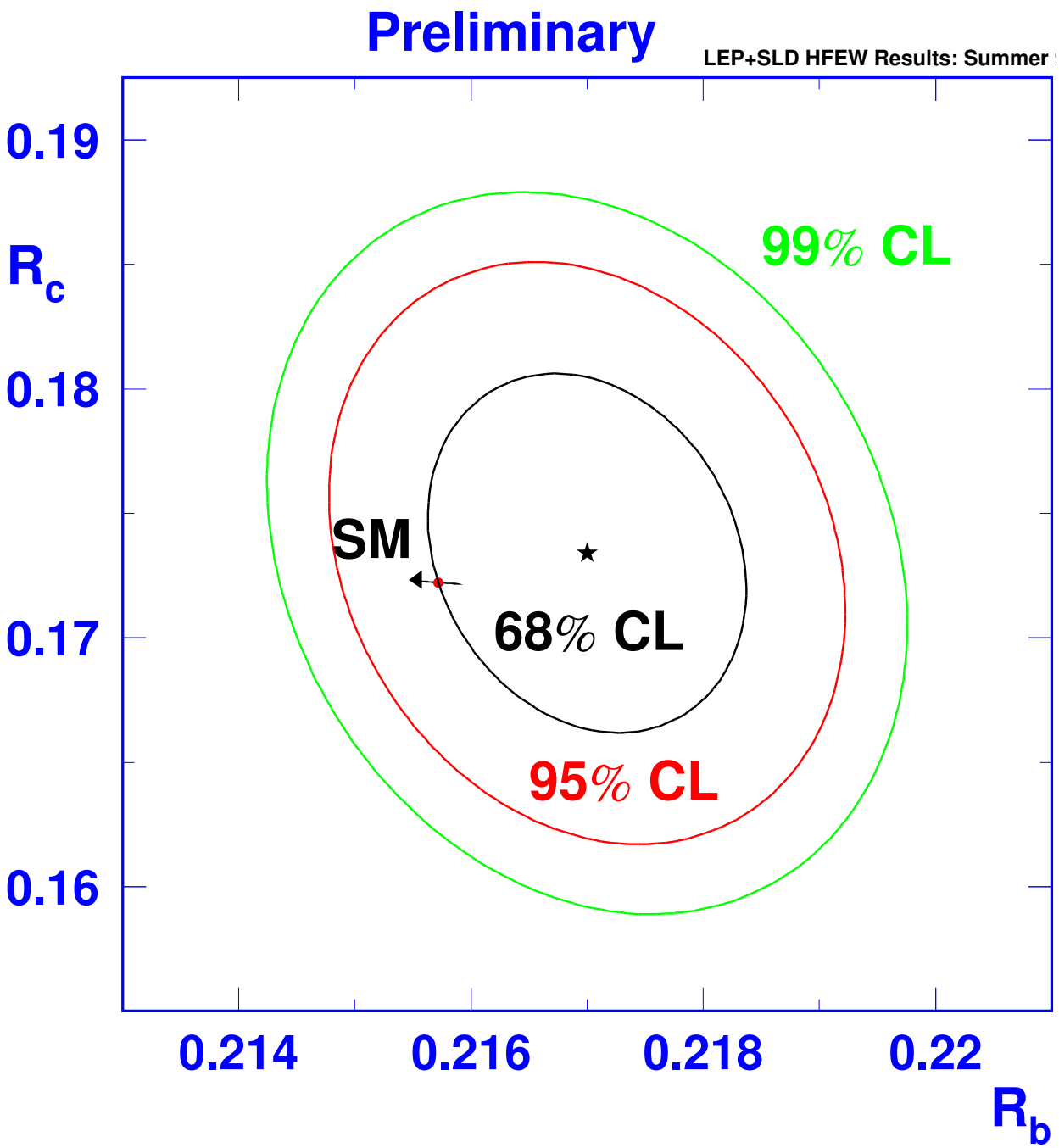

Figure 5: Contours in the R_b-R_c plane derived from the LEP and SLD data, corresponding to 68%, 95% and 99% confidence levels assuming Gaussian systematic errors. The Standard Model prediction for $m_t = 175.6 \pm 5.5$ GeV is also shown. The arrow points in the direction of increasing values of m_t.

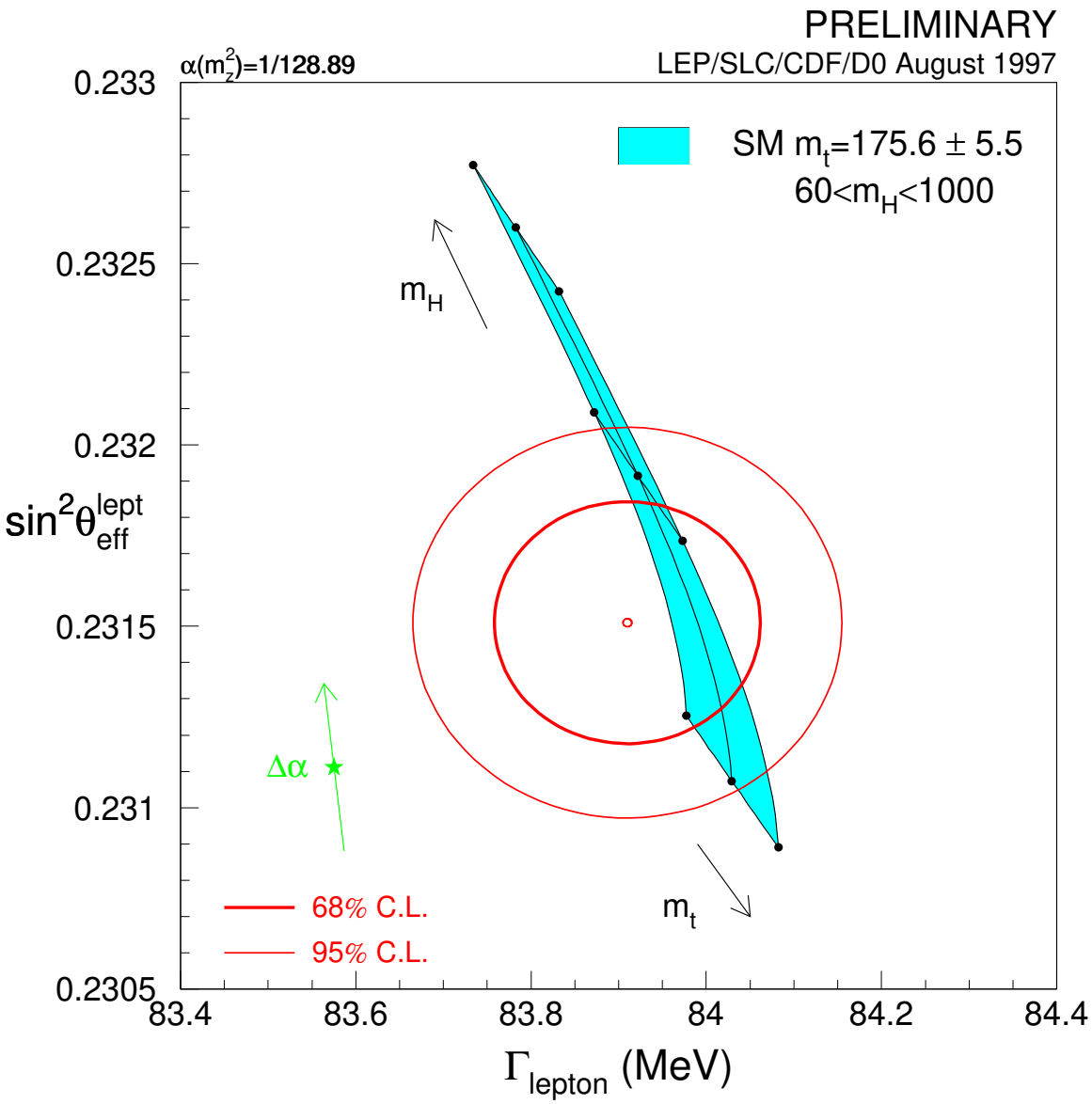

Figure 6: The LEP/SLD measurements of $\sin^2\theta^{\rm lept}_{\rm eff}$ (Table 23) and $\Gamma_{\ell\ell}$ (Table 9) and the Standard Model prediction. The star shows the predictions if among the electroweak radiative corrections only the photon vacuum polarisation is included. The corresponding arrow shows variation of this prediction if $\alpha(m_{\rm Z}^2)$ is changed by one standard deviation. This variation gives an additional uncertainty to the Standard Model prediction shown in the figure.

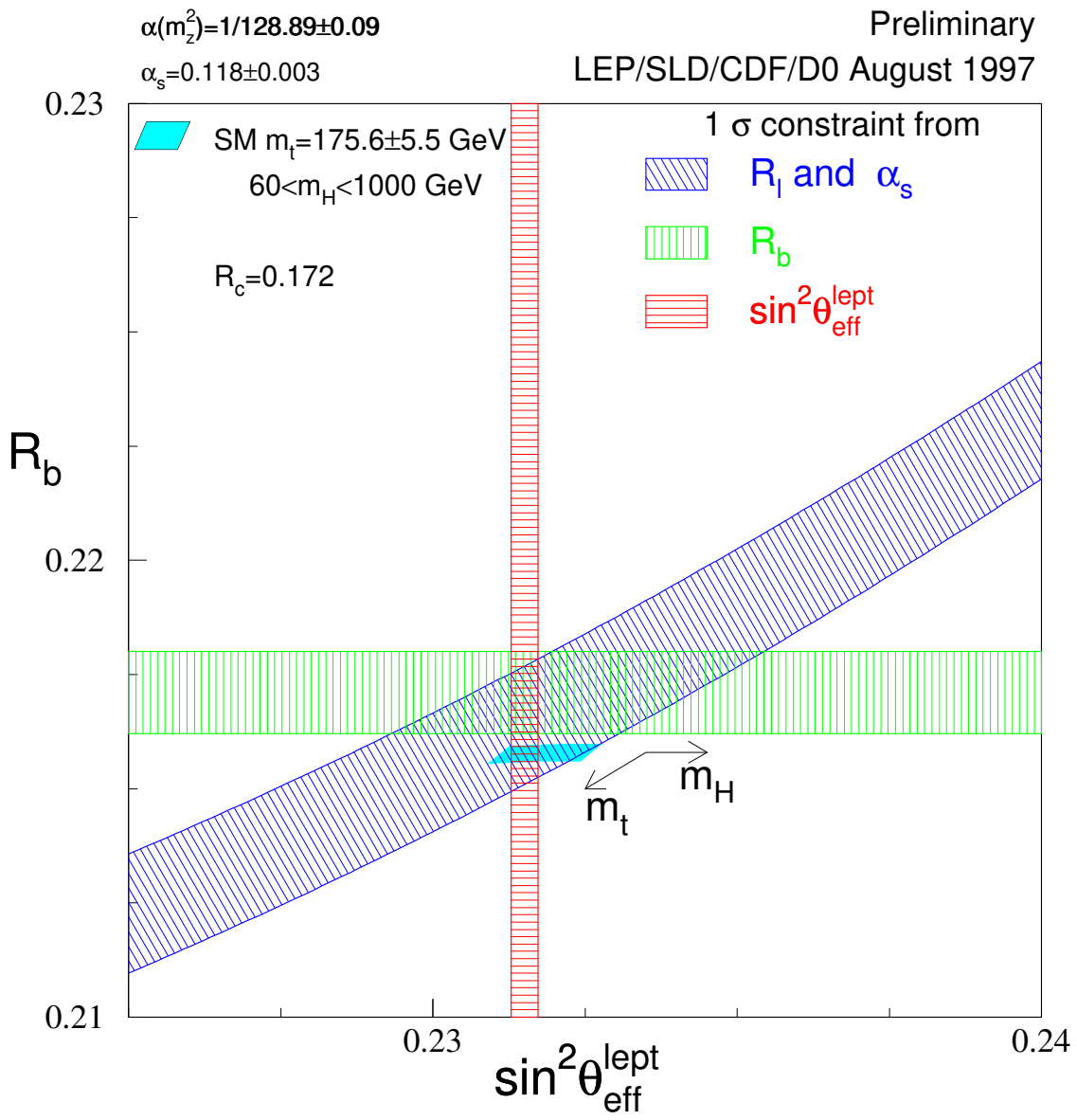

Figure 7: The LEP/SLD measurements of $\sin^2\theta^{\rm lept}_{\rm eff}$ (Table 23) and $R_{\rm b}(R_{\rm c} = 0.172)$ and the Standard Model prediction. Also shown is the constraint resulting from the measurement of R_ℓ on these variables, assuming $\alpha_s(m^2_{\rm Z}) = 0.118 \pm 0.003$, as well as the Standard Model dependence of light-quark partial widths on $\sin^2\theta^{\rm lept}_{\rm eff}$. The Standard Model value for $R_{\rm c}$ is assumed.

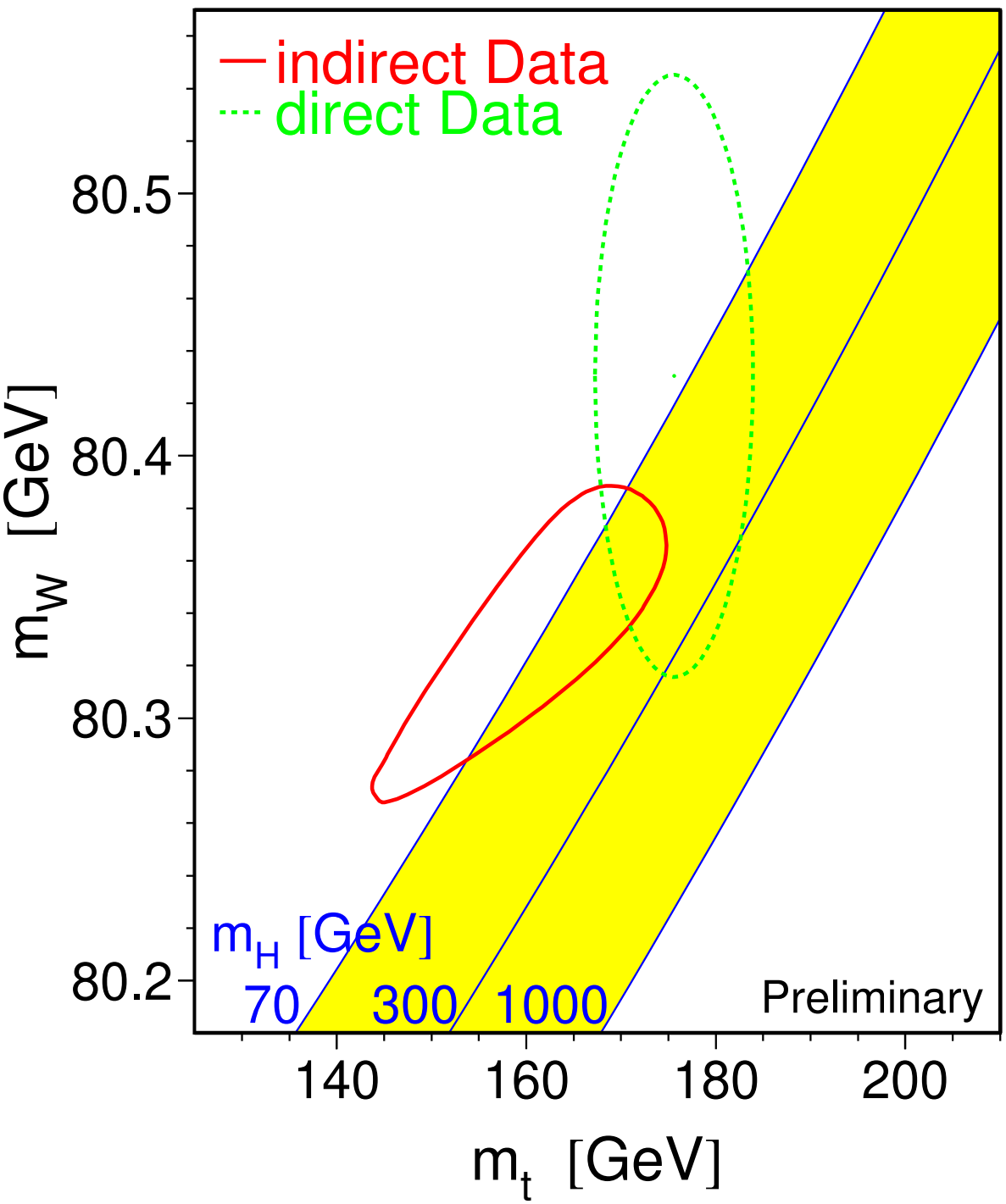

Figure 8: The comparison of the indirect measurements of m_{W} and m_{t} (LEP+SLD+νN data) (solid contour) and the direct measurements (Tevatron and LEPII data) (dashed contour). In both cases the 68% CL contours are plotted. Also shown is the Standard Model relationship for the masses as a function of the Higgs mass.

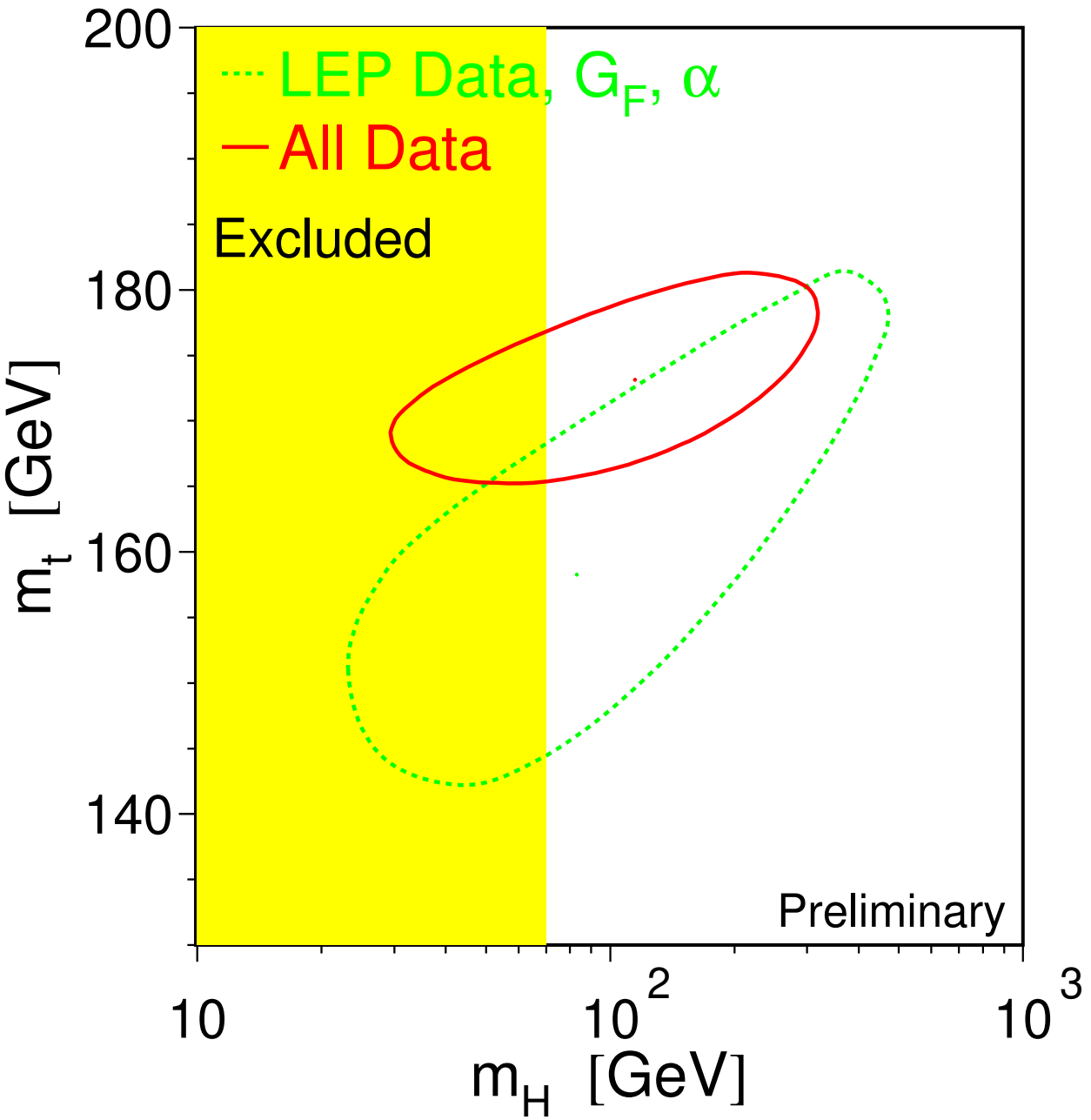

Figure 9: The 68% confidence level contours in m_{t} and m_{H} for the fits to LEP data only (dashed curve) and to all data including the CDF/DØ m_{t} measurement (solid curve).

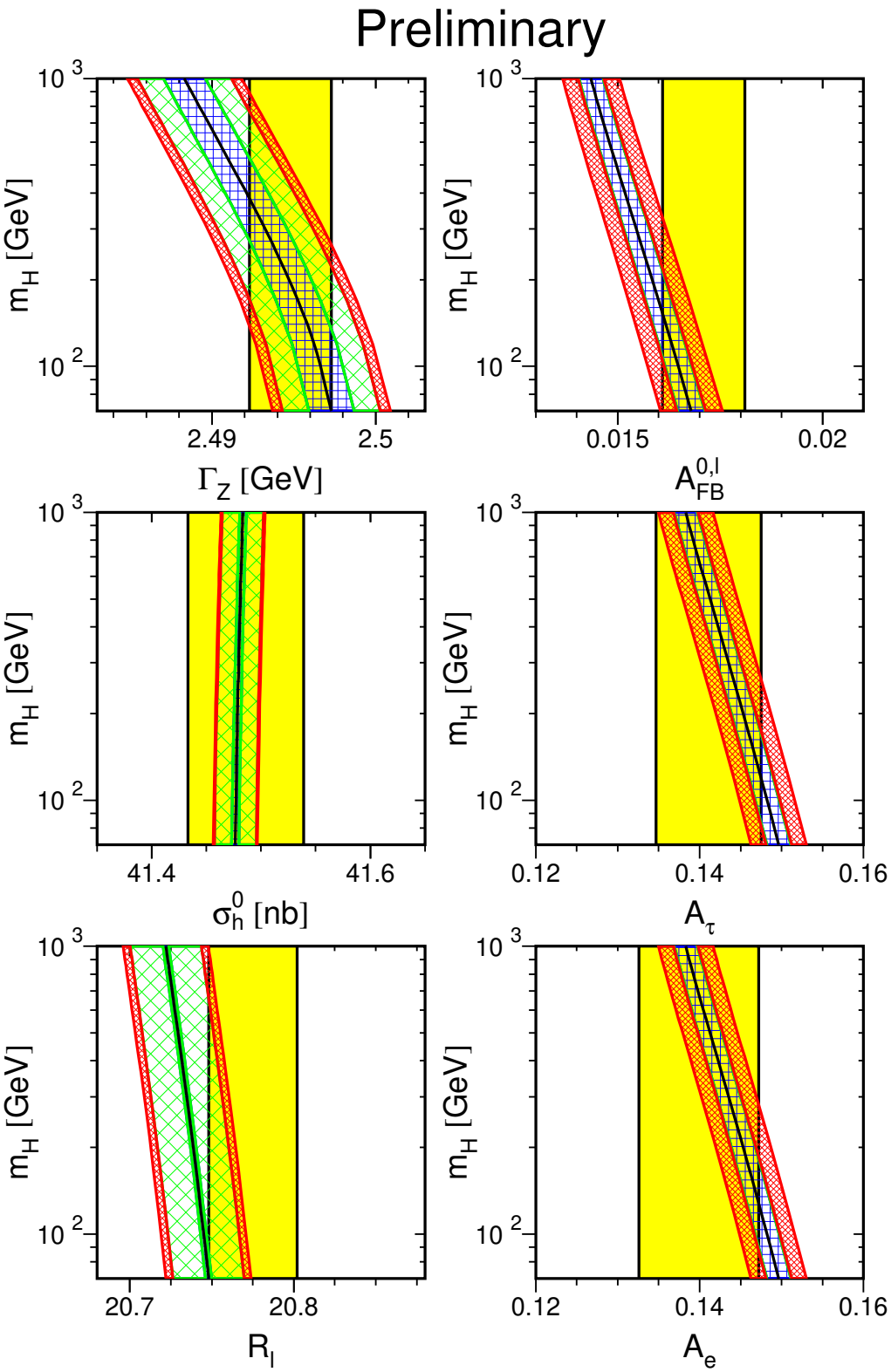

Figure 10: Comparison of LEP measurements with the Standard Model prediction as a function of m_{H}. The cross-hatch pattern parallel to the axes indicates the variation of the Standard Model prediction with $m_{\mathrm{t}} = 175.6 \pm 5.5$ GeV, the coarse diagonal cross-hatch pattern corresponds to a variation of $\alpha_s(m_{\mathrm{Z}}^2) = 0.118 \pm 0.003$, and the dense diagonal cross-hatching to the variation of $\alpha(m_{\mathrm{Z}}^2)^{-1} = 128.896 \pm 0.090$. The total width of the band corresponds to the linear sum of all uncertainties. The experimental errors on the parameters are indicated as vertical bands.

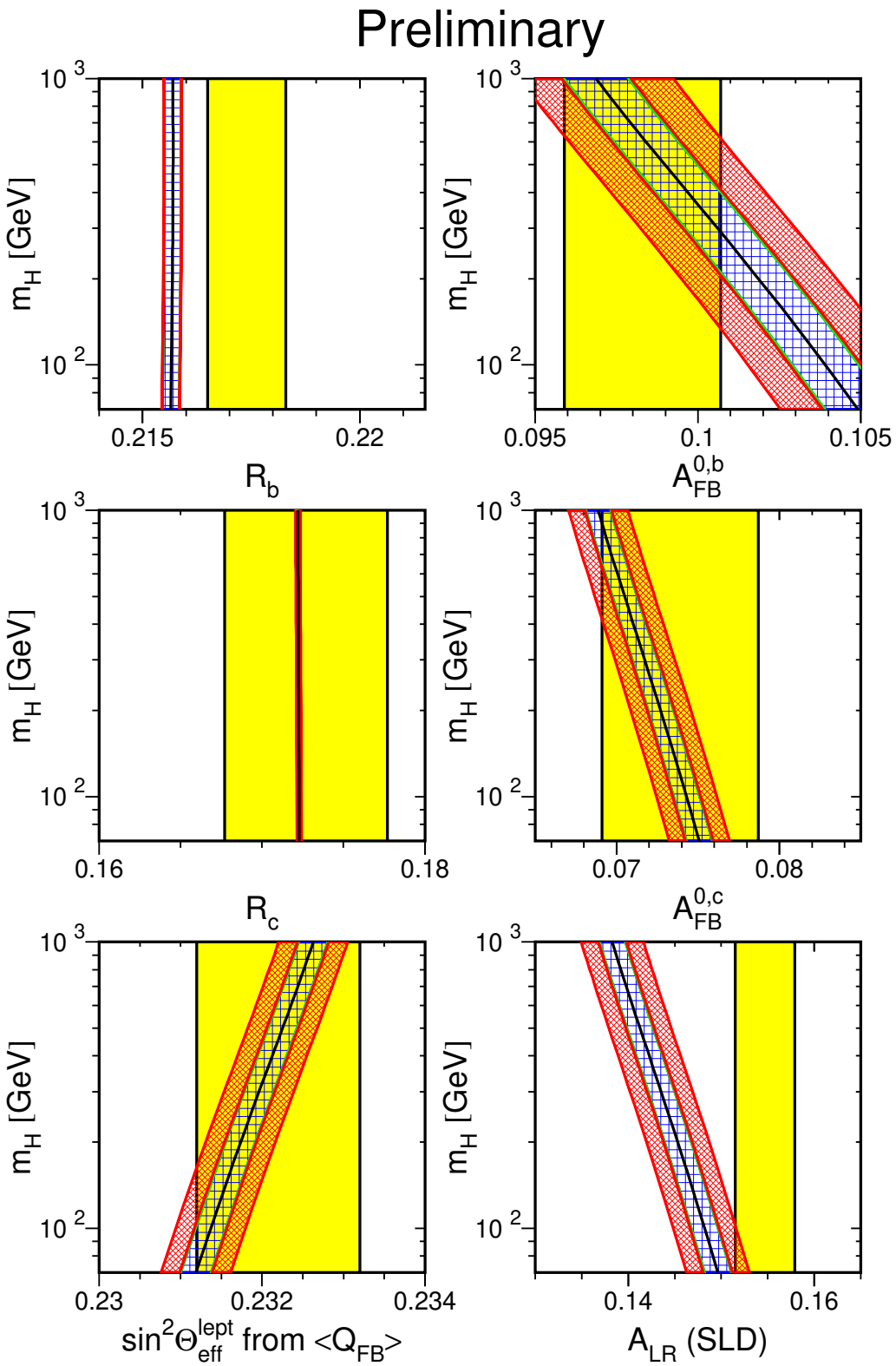

Figure 11: Comparison of LEP measurements with the Standard Model prediction as a function of m_{H} (*c.f.* Figure 10). For the comparison of R_{b} with the Standard Model the value of R_{c} has been fixed to its Standard Model prediction. Also shown is the comparison of the SLD measurement of A_{LR} with the Standard Model.

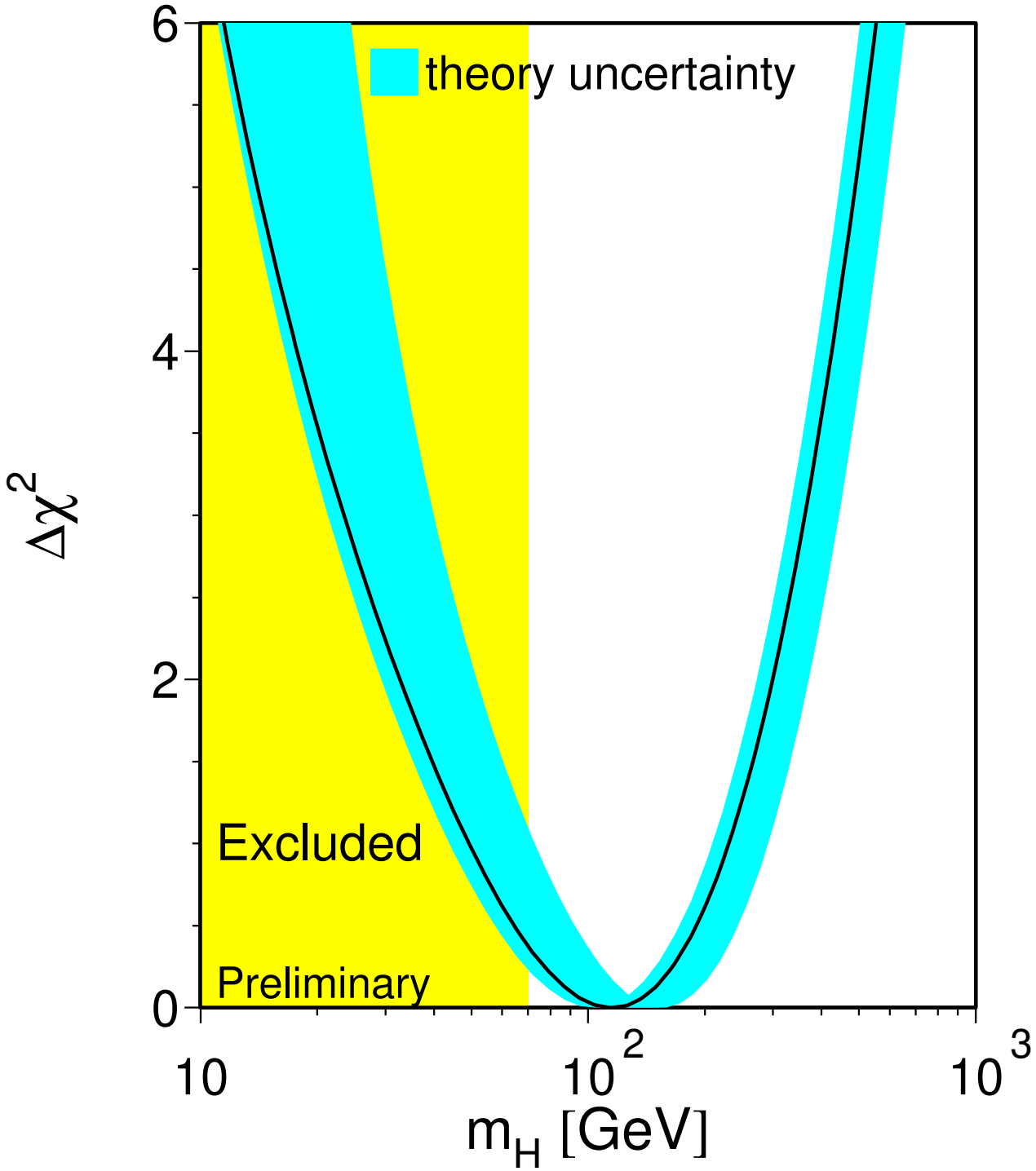

Figure 12: $\Delta\chi^2 = \chi^2 - \chi^2_{min}$ *vs.* $m_{\rm H}$ curve. The line is the result of the fit using all data (last column of Table 25); the band represents an estimate of the theoretical error due to missing higher order corrections.

Appendix

Heavy Flavour fit including off peak asymmetries

The full 17 parameter fit to the LEP and SLD data gave the following results:

$$
\begin{aligned}
R_{\mathrm{b}}^{0} &= 0.2170 \pm 0.0009 \\
R_{\mathrm{c}}^{0} &= 0.1733 \pm 0.0048 \\
A_{\mathrm{FB}}^{\mathrm{b\bar{b}}}(-2) &= 0.048 \pm 0.010 \\
A_{\mathrm{FB}}^{\mathrm{c\bar{c}}}(-2) &= -0.038 \pm 0.019 \\
A_{\mathrm{FB}}^{\mathrm{b\bar{b}}}(\mathrm{pk}) &= 0.0969 \pm 0.0025 \\
A_{\mathrm{FB}}^{\mathrm{c\bar{c}}}(\mathrm{pk}) &= 0.0681 \pm 0.0050 \\
A_{\mathrm{FB}}^{\mathrm{b\bar{b}}}(+2) &= 0.113 \pm 0.008 \\
A_{\mathrm{FB}}^{\mathrm{c\bar{c}}}(+2) &= 0.140 \pm 0.017 \\
\mathcal{A}_{\mathrm{b}} &= 0.900 \pm 0.058 \\
\mathcal{A}_{\mathrm{c}} &= 0.651 \pm 0.085 \\
\mathrm{BR}(\mathrm{b} \to \ell) &= 0.1112 \pm 0.0020 \\
\mathrm{BR}(\mathrm{b} \to \mathrm{c} \to \bar{\ell}) &= 0.0803 \pm 0.0033 \\
\overline{\chi} &= 0.1214 \pm 0.0043 \\
f(\mathrm{D}^{+}) &= 0.221 \pm 0.020 \\
f(\mathrm{D_s}) &= 0.112 \pm 0.027 \\
f(\mathrm{c}_{baryon}) &= 0.084 \pm 0.022 \\
\mathrm{P}(\mathrm{c} \to \mathrm{D}^{*+}) \times \mathrm{BR}(\mathrm{D}^{*+} \to \pi^{+}\mathrm{D}^{0}) &= 0.1609 \pm 0.0062
\end{aligned}
$$

with a χ^2/d.o.f. of $50/(94-17)$. The corresponding correlation matrix is given in Table 26. The energy for the peak-2, peak and peak$+2$ results are respectively 89.55 GeV, 91.26 GeV and 92.94 GeV. Note that the asymmetry results shown here are not the pole asymmetries which have been shown in Section 4.3.2.

	1) R_b	2) R_c	3) $A_{FB}^{b\bar{b}}$ (−2)	4) $A_{FB}^{c\bar{c}}$ (−2)	5) $A_{FB}^{b\bar{b}}$ (pk)	6) $A_{FB}^{c\bar{c}}$ (pk)	7) $A_{FB}^{b\bar{b}}$ (+2)	8) $A_{FB}^{c\bar{c}}$ (+2)	9) $\mathcal{A}_b$	10) $\mathcal{A}_c$	11) BR (1)	12) BR (2)	13) $\overline{\chi}$	14) $f(D^+)$	15) $f(D_s)$	16) $f(c_{bar.})$	17) PcDst
1)	1.00	−0.20	0.00	−0.01	−0.03	0.02	−0.01	0.01	−0.03	0.02	−0.09	−0.03	0.00	−0.18	−0.05	0.09	0.21
2)	−0.20	1.00	0.00	0.01	0.03	−0.07	0.01	−0.05	0.04	−0.04	0.09	0.13	0.01	−0.12	0.23	0.11	−0.58
3)	0.00	0.00	1.00	0.15	0.03	0.01	0.02	0.00	0.01	0.01	0.02	−0.03	0.08	0.00	0.00	0.00	0.00
4)	−0.01	0.01	0.15	1.00	0.02	0.02	0.01	0.00	0.00	0.00	0.01	−0.02	0.01	0.00	0.00	0.00	0.00
5)	−0.03	0.03	0.03	0.02	1.00	0.13	0.09	0.00	0.03	0.02	0.02	−0.15	0.24	−0.01	0.01	0.00	−0.02
6)	0.02	−0.07	0.01	0.02	0.13	1.00	0.00	0.14	0.00	0.07	0.13	−0.22	0.14	0.00	−0.01	0.00	0.04
7)	−0.01	0.01	0.02	0.01	0.09	0.00	1.00	0.14	0.01	0.00	0.00	−0.04	0.11	0.00	0.00	0.00	−0.01
8)	0.01	−0.05	0.00	0.00	0.00	0.14	0.14	1.00	0.00	0.03	0.06	−0.09	0.06	0.00	−0.01	0.00	0.03
9)	−0.03	0.04	0.01	0.00	0.03	0.00	0.01	0.00	1.00	0.08	0.01	−0.02	0.06	−0.01	0.01	0.01	−0.03
10)	0.02	−0.04	0.01	0.00	0.02	0.07	0.00	0.03	0.08	1.00	0.07	−0.18	0.10	−0.05	−0.02	0.02	0.02
11)	−0.09	0.09	0.02	0.01	0.02	0.13	0.00	0.06	0.01	0.07	1.00	−0.23	0.32	0.01	0.02	0.00	−0.06
12)	−0.03	0.13	−0.03	−0.02	−0.15	−0.22	−0.04	−0.09	−0.02	−0.18	−0.23	1.00	−0.39	0.01	0.03	0.00	−0.07
13)	0.00	0.01	0.08	0.01	0.24	0.14	0.11	0.06	0.06	0.10	0.32	−0.39	1.00	0.01	0.00	−0.01	−0.01
14)	−0.18	−0.12	0.00	0.00	−0.01	0.00	0.00	0.00	−0.01	−0.05	0.01	0.01	0.01	1.00	−0.31	−0.19	0.10
15)	−0.05	0.23	0.00	0.00	0.01	−0.01	0.00	−0.01	0.01	−0.02	0.02	0.03	0.00	−0.31	1.00	−0.25	−0.08
16)	0.09	0.11	0.00	0.00	0.00	0.00	0.00	0.00	0.01	0.02	0.00	0.00	−0.01	−0.19	−0.25	1.00	−0.04
17)	0.21	−0.58	0.00	0.00	−0.02	0.04	−0.01	0.03	−0.03	0.02	−0.06	−0.07	−0.01	0.10	−0.08	−0.04	1.00

Table 26: The correlation matrix for the set of the 17 heavy flavour parameters. BR(1) and BR(2) denote BR($b \to \ell$) and BR($b \to c \to \bar{\ell}$) respectively, PcDst denotes P($c \to D^{*+}$) × BR($D^{*+} \to \pi^+ D^0$).

The Measurements used in the Heavy Flavour Averages

In the following tables, preliminary results are indicated by the symbol "†." The values of centre-of-mass energy are given where relevant. In each table, the result used as input to the average procedure is given followed by the statistical error, the correlated and uncorrelated systematic errors, the total systematic error, and any dependence on other electroweak parameters. In the case of the asymmetries, the measurement moved to a common energy (89.55 GeV, 91.26 GeV and 92.94 GeV, respectively, for peak−2, peak and peak+2 results) is quoted as *corrected* asymmetry.

Contributions to the correlated systematic error quoted here are from any sources of error shared with one or more other results from different experiments in the same table, and the uncorrelated errors from the remaining sources. In the case of $\mathcal{A}_c$ and $\mathcal{A}_b$ from SLD the quoted correlated systematic error has contributions from any source shared with one or more other measurements from LEP experiment. Constants such as $a(x)$ denote the dependence on the assumed value of $x^{\rm used}$, which is also given.

	ALEPH		DELPHI		L3			OPAL		SLD
	92-95 multi [32]	90-91 lepton [24]	94† multi [33]	91-92 lepton [26]	94† multi [34]	91 shape [31]	90-91 lepton [28]	92-94 multi [35]	90-91 lepton [29]	93-95† multi [21]
R_b	0.2156	0.2162	0.2164	0.2146	0.2176	0.2220	0.2193	0.2175	0.2240	0.2124
Statistical	0.0009	0.0062	0.0008	0.0089	0.0015	0.0030	0.0081	0.0014	0.0110	0.0024
Uncorrelated	0.0007	0.0040	0.0006	0.0063	0.0014	0.0021	0.0047	0.0009	0.0045	0.0015
Correlated	0.0008	0.0031	0.0006	0.0020	0.0019	0.0061	0.0021	0.0012	0.0045	0.0006
Total Systematic	0.0011	0.0050	0.0009	0.0066	0.0023	0.0064	0.0051	0.0015	0.0063	0.0017
$a(R_c)$	-0.0033		-0.0041		-0.0364	-0.0209	-0.0232	-0.0183	-0.0132	-0.0068
$R_c^{\rm used}$	0.1720		0.1720		0.1722	0.1710	0.1710	0.1720	0.1710	0.1710
$a(\mathrm{BR}(b \to \ell))$						-0.0210				
$\mathrm{BR}(b \to \ell)^{\rm used}$						10.50				
$a(\mathrm{BR}(b \to c \to \bar{\ell}))$							0.0342			
$\mathrm{BR}(b \to c \to \bar{\ell})^{\rm used}$							7.90			
$a(f(D^+))$	-0.0010		-0.0011		-0.0087			-0.0032		-0.0007
$f(D^+)^{\rm used}$	0.2330		0.2330		0.2330			0.2350		0.2590
$a(f(D_s))$	-0.0001		0.0001		-0.0005			-0.0001		-0.0002
$f(D_s)^{\rm used}$	0.1020		0.1020		0.1020			0.0960		0.1150
$a(f(\Lambda_c))$	0.0002		0.0002		0.0008			0.0006		-0.0004
$f(\Lambda_c)^{\rm used}$	0.0650		0.0650		0.0650			0.0640		0.0740

Table 27: The measurements of R_b.

	ALEPH				DELPHI		OPAL		SLD
	90-91 lepton [24]	91-95† $D^{*\pm}$ [25]	91-95† c count [25]	92-95† lepton [25]	91-94† c count + $D^{*\pm}$ [38]	91-92 lepton [26]	90-95 $D^{*\pm}$ [39]	91-93 c count [39]	93-95† $D^{*\pm}$ [22]
R_c	0.1670	0.1724	0.1756	0.1649	0.1692	0.1640	0.1802	0.162	0.1810
Statistical	0.0054	0.0098	0.0048	0.0070	0.0080	0.0085	0.0098	0.011	0.0122
Uncorrelated	0.0149	0.0099	0.0085	0.0053	0.0071	0.0168	0.0100	0.009	0.0075
Correlated	0.0114	0.0013	0.0070	0.0092	0.0042	0.0114	0.0062	0.010	0.0024
Total Systematic	0.0188	0.0100	0.0110	0.0106	0.0083	0.0203	0.0118	0.020	0.0079
$a(R_b)$		-0.0022							-0.0215
R_b^{used}		0.2219							0.2155

Table 28: The measurements of R_c.

	ALEPH			DELPHI		L3	OPAL		
	90-95 lepton [24]	90-95 lepton [24]	90-95 lepton [24]	91-94† lepton [27]	91-94† $D^{*\pm}$ [27]	90-93† lepton [28]	91-95 jet [37]	90-95† lepton [29]	90-94† $D^{*\pm}$ [41]
$\sqrt{s}$ (GeV)	88.380	89.380	90.210	89.430	89.540	89.560	89.440	89.490	89.490
$A_{\rm FB}^{\rm b\bar{b}}(-2)$	-3.51	5.45	9.07	6.37	1.99	6.90	4.10	3.54	-8.70
$A_{\rm FB}^{\rm bb}(-2)$Corrected		5.01		6.66	2.01	6.99	4.36	3.68	-8.56
Statistical		1.80		3.86	10.48	3.50	2.10	1.73	10.80
Uncorrelated		0.04		0.16	1.12	0.34	0.25	0.16	2.53
Correlated		0.03		0.12	0.11	0.13	0.01	0.04	1.37
Total Systematic		0.05		0.19	1.12	0.37	0.25	0.16	2.88
$a(R_{\rm b})$		0.0870		-0.7233		-1.5984	-0.7300	-0.1000	
$R_{\rm b}^{\rm used}$		0.2192		0.2170		0.2160	0.2150	0.2155	
$a(R_{\rm c})$		0.0333		0.1221		0.9126	0.0700	0.1000	
$R_{\rm c}^{\rm used}$		0.1710		0.1710		0.1690	0.1730	0.1720	
$a(A_{\rm FB}^{\rm c\bar{c}}(-2))$		-0.186				-0.2684	-0.3156		
$A_{\rm FB}^{\rm c\bar{c}}(-2)^{\rm used}$		-2.34				-2.96	-2.81		
$a({\rm BR}({\rm b}\to\ell))$		-0.236		-0.9706		-0.7770		0.3406	
${\rm BR}({\rm b}\to\ell)^{\rm used}$		11.34		11.00		10.50		10.90	
$a({\rm BR}({\rm b}\to{\rm c}\to\bar{\ell}))$		-0.102		0.1580		-0.2464		-0.5298	
${\rm BR}({\rm b}\to{\rm c}\to\bar{\ell})^{\rm used}$		7.86		7.90		8.00		8.30	
$a(\overline{\chi})$		5.12		2.0533					
$\overline{\chi}^{\rm used}$		0.12460		0.12100					

Table 29: The measurements of $A_{\rm FB}^{\rm b\bar{b}}(-2)$.

	ALEPH	DELPHI			L3		OPAL		
	90-95 lepton [24]	91-94† lepton [27]	91-94† $D^{*\pm}$ [27]	91-94† jet [27]	94† jet [36]	90-95† lepton [28]	91-95 jet [37]	90-95† lepton [29]	90-94† $D^{*\pm}$ [41]
$\sqrt{s}$ (GeV)	91.210	91.230	91.230	91.230	91.220	91.260	91.210	91.240	91.240
$A_{\rm FB}^{\rm b\bar{b}}({\rm pk})$	9.88	10.75	7.23	9.95	8.55	9.63	10.04	9.10	9.50
$A_{\rm FB}^{\rm bb}({\rm pk})$Corrected	9.97	10.81	7.29	10.01	8.63	9.63	10.13	9.14	9.54
Statistical	0.46	0.77	2.50	0.72	1.18	0.65	0.52	0.44	2.70
Uncorrelated	0.10	0.21	1.25	0.38	0.46	0.28	0.41	0.14	2.15
Correlated	0.16	0.23	0.11	0.12	0.32	0.22	0.20	0.15	0.47
Total Systematic	0.19	0.31	1.25	0.40	0.56	0.35	0.46	0.20	2.20
$a(R_{\rm b})$	-1.4613	-2.8933		-0.6000	-8.2916	-2.0736	-7.6300	-0.7000	
$R_{\rm b}^{\rm used}$	0.2192	0.2170		0.2210	0.2182	0.2160	0.2150	0.2155	
$a(R_{\rm c})$	1.0474	1.2214		0.2400	1.0925	1.2506	0.4600	0.6000	
$R_{\rm c}^{\rm used}$	0.1710	0.1710		0.1710	0.1707	0.1690	0.1730	0.1720	
$a(A_{\rm FB}^{\rm c\bar{c}}({\rm pk}))$	0.5068				1.1185	0.6253	0.6870		
$A_{\rm FB}^{\rm c\bar{c}}({\rm pk})^{\rm used}$	6.41				6.21	6.70	6.19		
$a({\rm BR}({\rm b}\to\ell))$	-1.3500	-3.5588				-1.5540		-0.3406	
${\rm BR}({\rm b}\to\ell)^{\rm used}$	11.34	11.00				10.50		10.90	
$a({\rm BR}({\rm b}\to{\rm c}\to\bar{\ell}))$	-0.1886	0.4740				-0.0272		-0.3532	
${\rm BR}({\rm b}\to{\rm c}\to\bar{\ell})^{\rm used}$	7.86	7.90				8.00		8.30	
$a(\overline{\chi})$	3.2930	3.5200							
$\overline{\chi}^{\rm used}$	0.12460	0.12100							

Table 30: The measurements of $A_{\rm FB}^{\rm b\bar{b}}({\rm pk})$.

	ALEPH			DELPHI		L3	OPAL		
	90-95 lepton [24]	90-95 lepton [24]	90-95 lepton [24]	91-94† lepton [27]	91-94† $D^{*\pm}$ [27]	90-93† lepton [28]	91-95 jet [37]	90-95† lepton [29]	90-94† $D^{*\pm}$ [41]
$\sqrt{s}$ (GeV)	92.050	92.940	93.900	93.017	92.940	92.930	92.910	92.950	92.950
$A_{\rm FB}^{\rm b\bar{b}}(+2)$	3.91	10.56	9.00	15.23	5.70	10.80	14.60	10.70	-2.10
$A_{\rm FB}^{\rm bb}(+2)$Corrected	10.00			15.15	5.70	10.98	14.63	10.69	-2.11
Statistical	1.50			3.65	9.55	2.90	1.70	1.43	9.00
Uncorrelated	0.14			0.50	1.61	0.35	0.72	0.25	2.18
Correlated	0.22			0.41	0.11	0.15	0.06	0.28	1.59
Total Systematic	0.26			0.65	1.62	0.38	0.72	0.37	2.70
$a(R_{\rm b})$	-1.86			-2.8933		-1.5984	-12.9000	-0.8000	
$R_{\rm b}^{\rm used}$	0.2192			0.2170		0.2160	0.2150	0.2155	
$a(R_{\rm c})$	1.43			-0.9771		0.9126	0.6900	0.8000	
$R_{\rm c}^{\rm used}$	0.1710			0.1710		0.1690	0.1730	0.1720	
$a(A_{\rm FB}^{\rm c\bar{c}}(+2))$	0.913					1.1156	1.3287		
$A_{\rm FB}^{\rm c\bar{c}}(+2)^{\rm used}$	12.51					12.13	12.08		
$a({\rm BR}({\rm b}\to\ell))$	-1.65			-3.2353		-0.4200		-1.3625	
${\rm BR}({\rm b}\to\ell)^{\rm used}$	11.34			11.00		10.50		10.90	
$a({\rm BR}({\rm b}\to{\rm c}\to\bar{\ell}))$	-0.2410			0.4740		-0.5280		0.7064	
${\rm BR}({\rm b}\to{\rm c}\to\bar{\ell})^{\rm used}$	7.86			7.90		8.00		8.30	
$a(\overline{\chi})$	6.409			4.8400					
$\overline{\chi}^{\rm used}$	0.12460			0.12100					

Table 31: The measurements of $A_{\rm FB}^{\rm b\bar{b}}(+2)$.

	ALEPH	DELPHI	OPAL	
	91-94† $D^{*\pm}$ [40]	91-94† $D^{*\pm}$ [27]	90-95† lepton [29]	90-94† $D^{*\pm}$ [41]
$\sqrt{s}$ (GeV)	89.400	89.540	89.490	89.490
$A_{\rm FB}^{\rm c\bar{c}}(-2)$	-4.93	0.20	-6.90	3.90
$A_{\rm FB}^{\rm c\bar{c}}(-2)$Corrected	-4.03	0.26	-6.54	4.26
Statistical	7.60	5.19	2.44	5.10
Uncorrelated	0.84	0.55	0.43	0.80
Correlated	0.04	0.07	0.21	0.30
Total Systematic	0.84	0.55	0.48	0.86
$a(R_{\rm b})$			-3.4000	
$R_{\rm b}^{\rm used}$			0.2155	
$a(R_{\rm c})$			3.2000	
$R_{\rm c}^{\rm used}$			0.1720	
$a(A_{\rm FB}^{\rm b\bar{b}}(-2))$	0.2295			
$A_{\rm FB}^{\rm b\bar{b}}(-2)^{\rm used}$	-1.34			
$a({\rm BR}({\rm b}\to\ell))$			-1.7031	
${\rm BR}({\rm b}\to\ell)^{\rm used}$			10.90	
$a({\rm BR}({\rm b}\to{\rm c}\to\bar{\ell}))$			-1.4128	
${\rm BR}({\rm b}\to{\rm c}\to\bar{\ell})^{\rm used}$			8.30	

Table 32: The measurements of $A_{\rm FB}^{\rm c\bar{c}}(-2)$.

	ALEPH		DELPHI		L3	OPAL	
	90-91 lepton [24]	91-94† $D^{*\pm}$ [40]	91-94† lepton [27]	91-94† $D^{*\pm}$ [27]	90-91 lepton [28]	90-95† lepton [29]	90-94† $D^{*\pm}$ [41]
$\sqrt{s}$ (GeV)	91.260	91.200	91.230	91.230	91.240	91.240	91.240
$A_{\rm FB}^{\rm c\bar{c}}({\rm pk})$	9.30	6.44	8.39	7.64	7.84	5.95	6.30
$A_{\rm FB}^{\rm c\bar{c}}({\rm pk})$Corrected	9.30	6.73	8.54	7.79	8.02	6.05	6.40
Statistical	2.00	1.30	1.40	1.21	3.70	0.59	1.20
Uncorrelated	1.55	0.20	0.91	0.55	2.42	0.37	0.53
Correlated	1.04	0.17	0.74	0.09	0.60	0.38	0.15
Total Systematic	1.86	0.26	1.18	0.55	2.50	0.53	0.55
$a(R_{\rm b})$			3.6167		4.3200	4.1000	
$R_{\rm b}^{\rm used}$			0.2170		0.2160	0.2155	
$a(R_{\rm c})$			-6.3514		-6.7600	-3.8000	
$R_{\rm c}^{\rm used}$			0.1710		0.1690	0.1720	
$a(A_{\rm FB}^{\rm b\bar{b}}({\rm pk}))$		-1.5110			6.4274		
$A_{\rm FB}^{\rm b\bar{b}}({\rm pk})^{\rm used}$		8.81			8.84		
$a({\rm BR}({\rm b}\to\ell))$			4.8529		3.5007	5.1094	
${\rm BR}({\rm b}\to\ell)^{\rm used}$			11.00		10.50	10.90	
$a({\rm BR}({\rm b}\to{\rm c}\to\bar{\ell}))$			-3.7920		-3.2917	-1.7660	
${\rm BR}({\rm b}\to{\rm c}\to\bar{\ell})^{\rm used}$			7.90		7.90	8.30	

Table 33: The measurements of $A_{\rm FB}^{\rm c\bar{c}}({\rm pk})$.

	ALEPH	DELPHI	OPAL	
	91-94† $D^{*\pm}$ [40]	91-94† $D^{*\pm}$ [27]	90-95† lepton [29]	90-94† $D^{*\pm}$ [41]
$\sqrt{s}$ (GeV)	93.000	92.940	92.950	92.950
$A_{\rm FB}^{\rm c\bar{c}}(+2)$	10.97	8.10	15.60	15.80
$A_{\rm FB}^{\rm c\bar{c}}(+2)$Corrected	10.81	8.10	15.57	15.77
Statistical	6.10	4.55	2.02	4.10
Uncorrelated	0.71	0.55	0.89	1.05
Correlated	0.25	0.15	0.37	0.21
Total Systematic	0.75	0.57	0.96	1.07
$a(R_{\rm b})$			9.6000	
$R_{\rm b}^{\rm used}$			0.2155	
$a(R_{\rm c})$			-8.9000	
$R_{\rm c}^{\rm used}$			0.1720	
$a(A_{\rm FB}^{\rm b\bar{b}}(+2))$	-2.0639			
$A_{\rm FB}^{\rm b\bar{b}}(+2)^{\rm used}$	12.04			
$a({\rm BR}({\rm b}\to\ell))$			9.5375	
${\rm BR}({\rm b}\to\ell)^{\rm used}$			10.90	
$a({\rm BR}({\rm b}\to{\rm c}\to\bar{\ell}))$			-1.5894	
${\rm BR}({\rm b}\to{\rm c}\to\bar{\ell})^{\rm used}$			8.30	

Table 34: The measurements of $A_{\rm FB}^{\rm c\bar{c}}(+2)$.

	SLD		
	93-95† lepton [23]	93-95† jet [23]	93-95† $K^{\pm}$ [23]
$\sqrt{s}$ (GeV)	91.280	91.280	91.260
$\mathcal{A}_{\rm b}$	0.877	0.911	0.891
Statistical	0.068	0.045	0.083
Uncorrelated	0.038	0.044	0.113
Correlated	0.022	0.002	0.002
Total Systematic	0.044	0.044	0.113
$a(R_{\rm b})$	-0.4302	-0.0442	-0.0139
$R_{\rm b}^{\rm used}$	0.2216	0.2158	0.2180
$a(R_{\rm c})$	0.0800	0.1103	0.0077
$R_{\rm c}^{\rm used}$	0.1600	0.1715	0.1710
$a(\mathcal{A}_{\rm c})$		0.0611	-0.0609
$\mathcal{A}_{\rm c}^{\rm used}$		0.670	0.666
$a({\rm BR}({\rm b}\to\ell))$	-0.3176		
${\rm BR}({\rm b}\to\ell)^{\rm used}$	10.75		
$a({\rm BR}({\rm b}\to{\rm c}\to\bar{\ell}))$	0.1125		
${\rm BR}({\rm b}\to{\rm c}\to\bar{\ell})^{\rm used}$	8.10		
$a(\overline{\chi})$	0.3677		
$\overline{\chi}^{\rm used}$	0.12170		

Table 35: The measurements of $\mathcal{A}_{\rm b}$.

	SLD		
	93-95† lepton [23]	93-95† $D^{*\pm}$ [23]	93-95† K+vertex [23]
$\sqrt{s}$ (GeV)	91.280	91.260	91.260
$\mathcal{A}_c$	0.614	0.640	0.662
Statistical	0.104	0.110	0.066
Uncorrelated	0.040	0.053	0.040
Correlated	0.050	0.020	0.002
Total Systematic	0.064	0.057	0.040
$a(R_b)$	0.1173		
$R_b^{\rm used}$	0.2216		
$a(R_c)$	-0.4112		
$R_c^{\rm used}$	0.1600		
$a(\mathcal{A}_b)$		-0.1278	-0.0467
$\mathcal{A}_b{}^{\rm used}$		0.935	0.935
$a(\mathrm{BR}(b \to \ell))$	0.4007		
$\mathrm{BR}(b \to \ell)^{\rm used}$	10.75		
$a(\mathrm{BR}(b \to c \to \bar{\ell}))$	-0.5287		
$\mathrm{BR}(b \to c \to \bar{\ell})^{\rm used}$	8.10		
$a(\overline{\chi})$			0.0910
$\overline{\chi}^{\rm used}$			0.13000
$a(f(D^+))$			-0.0832
$f(D^+)^{\rm used}$			0.2590
$a(f(D_s))$			-0.0155
$f(D_s)^{\rm used}$			0.1150
$a(f(\Lambda_c))$			0.0026
$f(\Lambda_c)^{\rm used}$			0.0740

Table 36: The measurements of $\mathcal{A}_c$.

	ALEPH		DELPHI		L3		OPAL
	90-91 lepton [24]	92-93† multi [24]	91-92 lepton [26]	94† multi [30]	90-91 lepton [28]	92 lepton [28]	90-91 lepton [29]
BR(b $\to \ell$)	11.20	11.01	11.30	10.64	11.42	10.68	10.60
Statistical	0.33	0.10	0.45	0.13	0.48	0.11	0.60
Uncorrelated	0.32	0.20	0.50	0.24	0.30	0.36	0.39
Correlated	0.27	0.21	0.46	0.36	0.21	0.26	0.53
Total Systematic	0.42	0.29	0.68	0.43	0.37	0.44	0.66
$a(R_{\rm b})$						-9.2571	
$R_{\rm b}^{\rm used}$						0.2160	
$a(R_{\rm c})$				0.2756	0.6107		0.2236
$R_{\rm c}^{\rm used}$				0.1715	0.1710		0.1710
$a(\mathrm{BR(b \to c \to \bar{\ell})})$					0.4608	-1.1700	
$\mathrm{BR(b \to c \to \bar{\ell})}^{\rm used}$					7.90	9.00	
$a(\overline{\chi})$		0.2075					
$\overline{\chi}^{\rm used}$		0.12610					

Table 37: The measurements of BR(b $\to \ell$).

	ALEPH		DELPHI		OPAL
	90-91 lepton [24]	92-93† multi [24]	91-92 lepton [26]	94† multi [30]	90-91 lepton [29]
BR(b $\to$ c $\to \bar{\ell}$)	8.81	7.68	7.90	8.32	8.40
Statistical	0.25	0.18	0.49	0.29	0.40
Uncorrelated	0.40	0.25	0.95	0.40	0.57
Correlated	0.69	0.42	0.78	0.63	0.38
Total Systematic	0.80	0.49	1.23	0.75	0.68
$a(R_{\rm c})$				0.0919	0.3157
$R_{\rm c}^{\rm used}$				0.1715	0.1710
$a(\overline{\chi})$		-0.5108			
$\overline{\chi}^{\rm used}$		0.12610			

Table 38: The measurements of BR(b $\to$ c $\to \bar{\ell}$).

	ALEPH	DELPHI		L3	OPAL
	90-95 lepton [24]	91-92 lepton [26]	94† lepton [30]	90-93 lepton [28]	90-95† lepton [29]
$\overline{\chi}$	0.12461	0.14900	0.12700	0.11870	0.11390
Statistical	0.00515	0.02000	0.01600	0.00680	0.00540
Uncorrelated	0.00244	0.01044	0.00248	0.00453	0.00306
Correlated	0.00403	0.01192	0.00506	0.00257	0.00324
Total Systematic	0.00471	0.01584	0.00563	0.00521	0.00446
$a(R_{\mathrm{b}})$	0.0341			0.0004	
$R_{\mathrm{b}}^{\mathrm{used}}$	0.2192			0.2160	
$a(R_{\mathrm{c}})$	0.0009		-0.0031	0.0003	
$R_{\mathrm{c}}^{\mathrm{used}}$	0.1710		0.1715	0.1690	
$a(\mathrm{BR}(\mathrm{b} \to \ell))$	0.0524			0.0521	0.0170
$\mathrm{BR}(\mathrm{b} \to \ell)^{\mathrm{used}}$	11.34			10.50	10.90
$a(\mathrm{BR}(\mathrm{b} \to \mathrm{c} \to \bar{\ell}))$	-0.0440			-0.0427	-0.0318
$\mathrm{BR}(\mathrm{b} \to \mathrm{c} \to \bar{\ell})^{\mathrm{used}}$	7.86			8.00	8.30

Table 39: The measurements of $\overline{\chi}$.

	DELPHI	OPAL
	91-94† $\mathrm{D}^{*\pm}$ [38]	90-95 $\mathrm{D}^{*\pm}$ [39]
$\mathrm{P}(\mathrm{c} \to \mathrm{D}^{*+}) \times \mathrm{BR}(\mathrm{D}^{*+} \to \pi^+\mathrm{D}^0)$	0.1678	0.1516
Statistical	0.0069	0.0096
Uncorrelated	0.0065	0.0085
Correlated	0.0011	0.0026
Total Systematic	0.0066	0.0089

Table 40: The measurements of $\mathrm{P}(\mathrm{c} \to \mathrm{D}^{*+}) \times \mathrm{BR}(\mathrm{D}^{*+} \to \pi^+\mathrm{D}^0)$.

References

[1] The LEP Collaborations ALEPH, DELPHI, L3, OPAL the LEP Electroweak Working Group, and the SLD Heavy Flavour Group, *A Combination of Preliminary LEP Electroweak Measurements and Constraints on the Standard Model*, CERN-PPE/96-183.

[2] LEP Electroweak Working Group, *An Investigation of the Interference between Photon and Z-Boson Exchange*, Internal Note, LEPEWWG/LS/97-02, in preparation.

[3] The LEP Collaborations ALEPH, DELPHI, L3, OPAL and the LEP Electroweak Working Group, *Combined Preliminary Data on* Z *Parameters from the LEP Experiments and Constraints on the Standard Model*, CERN-PPE/94-187.

[4] The LEP Experiments: Aleph, Delphi, L3 and Opal, Nucl. Inst. Meth. **A378** (1996) 101.

[5] ALEPH Collaboration, D. Decamp *et al.*, Z. Phys. **C48** (1990) 365;
ALEPH Collaboration, D. Decamp *et al.*, Z. Phys. **C53** (1992) 1;
ALEPH Collaboration, D. Buskulic *et al.*, Z. Phys. **C60** (1993) 71;
ALEPH Collaboration, D. Buskulic *et al.*, Z. Phys. **C62** (1994) 539;
ALEPH Collaboration, *Preliminary Results on Z Production Cross Section and Lepton Forward-Backward Asymmetries using the 1990-1995 Data*, contributed paper to ICHEP96, Warsaw, 25-31 July 1996, **PA-07-069**; updated for EPS-HEP-97, Jerusalem.

[6] DELPHI Collaboration, P. Aarnio *et al.*, Nucl. Phys. **B367** (1991) 511;
DELPHI Collaboration, P. Abreu *et al.*, Nucl. Phys. **B417** (1994) 3;
DELPHI Collaboration, P. Abreu *et al.*, Nucl. Phys. **B418** (1994) 403;
DELPHI Collaboration, DELPHI Note 95-62 PHYS 497, July 1995;
DELPHI Collaboration, DELPHI Note 97-130 CONF 109, contributed paper to EPS-HEP-97, Jerusalem, **EPS-463**.

[7] L3 Collaboration, B. Adeva *et al.*, Z. Phys. **C51** (1991) 179;
L3 Collaboration, O. Adriani *et al.*, Phys. Rep. **236** (1993) 1;
L3 Collaboration, M. Acciarri *et al.*, Z. Phys. **C62** (1994) 551;
L3 Collaboration, *Preliminary L3 Results on Electroweak Parameters using 1990-96 Data*, L3 Note 2065, March 1997, available via http://hpl3sn02.cern.ch/note/note-2065.ps.gz.

[8] OPAL Collaboration, G. Alexander *et al.*, Z. Phys. **C52** (1991) 175;
OPAL Collaboration, P.D. Acton *et al.*, Z. Phys. **C58** (1993) 219;
OPAL Collaboration, R. Akers *et al.*, Z. Phys. **C61** (1994) 19;
OPAL Collaboration, *A Preliminary Update of the* Z *Line Shape and Lepton Asymmetry Measurements with the 1993 and 1994 Data*, OPAL Physics Note PN166, Febuary 1995;
OPAL Collaboration, *The Preliminary OPAL SiW luminosity analysis: Results for the 1994 Summer conferences*, OPAL Physics Note PN142, July 1994;
OPAL Collaboration, *A Preliminary Update of the Z Line Shape and Lepton Asymmetry Measurements with a Revised 1993-1994 LEP Energy and 1995 Lepton Asymmetry*, OPAL Physics Note PN242, July 1996;
OPAL Collaboration, *Measurements of Lepton Pair Asymmetries using the 1995 Data*, contributed paper to ICHEP96, Warsaw, 25-31 July 1996 **PA07-015**;
OPAL Collaboration, *A Preliminary Update of the Z Lineshape and Lepton Asymmetry Measurements with the 1995 Data*, OPAL Physics Note PN286, March 1997.

[9] A. Arbuzov, *et al.*, Phys. Lett. **B383** (1996) 238;
S. Jadach, *et al.*, *Update of the Monte Carlo program BHLUMI for Bhabha scattering at*

low angles to version 4.04, CERN-TH/96-156, UTHEP-96-0601, June 1996, submitted to Comp. Phys. Comm.
The BHLUMI 4.04 program is available from http://hpjmiady.ifj.edu.pl.

[10] S. Jadach, E. Richter-Wąs, B.F.L. Ward and Z. Wąs, Phys. Lett. **B353** (1995) 362.

[11] The LEP Collaborations ALEPH, DELPHI, L3, OPAL and the LEP Electroweak Working Group, *Updated Parameters of the* Z *Resonance from Combined Preliminary Data of the LEP Experiments*, CERN-PPE/93-157.

[12] See, for example, M. Consoli *et al.*, in "Z Physics at LEP 1", CERN Report CERN 89-08 (1989), eds G. Altarelli, R. Kleiss and C. Verzegnassi, Vol. 1, p. 7.

[13] LEP Energy Working Group note 96-07, E. Lancon and A. Blondel, *Determination of the LEP Energy Spread Using Experimental Constraints.*

[14] LEP Energy Working Group, private communication. The contact person is Tiziano Camporesi, mail address T.Camporesi@cern.ch.

[15] G. Wilkinson, *The determination of the LEP energy in the 1995 Z^0 scan*, talk presented at ICHEP96, Warsaw, 25-31 July 1996, to appear in the proceedings.

[16] ALEPH Collaboration, D. Buskulic *et al.*, Zeit. Phys. **C69** (1996) 183.

[17] DELPHI Collaboration, P. Abreu *et al.*, Z. Phys. **C67** (1995) 183;
DELPHI Collaboration, *An updated measurement of tau polarisation*, DELPHI 96-114 CONF 42, contributed paper to ICHEP96, Warsaw, 25-31 July 1996, **PA07-008**.

[18] L3 Collaboration, O. Acciari *et al.*, Phys. Lett. **B341** (1994) 245;
L3 Collaboartion, *Measurement of the τ Polarization and the Spin Correlations in* $e^+e^- \to \tau^+\tau^-$, L3 note 2131, contributed paper to EPS-HEP-97, Jerusalem, **EPS-481**.

[19] OPAL Collaboration, G.Alexander *et al.*, *A Precise Measurement of the Tau Polarization and its Forward-Backward Asymmetry at LEP* CERN-PPE/96-078, submitted to Z. Phys. C.

[20] The LEP Heavy Flavour Group, *Presentation of LEP Electroweak Heavy Flavour Results for Summer 1996 Conferences*, LEPHF/96-01, ALEPH Note 96-099, DELPHI 96–67 PHYS 627, L3 Note 1969, OPAL Technical Note TN391.

[21] SLD Collaboration, SLAC-PUB-7585, contributed paper to EPS-HEP-97, Jerusalem, **EPS-118**.

[22] SLD Collaboration, SLAC-PUB-7594, contributed paper to EPS-HEP-97, Jerusalem, **EPS-120**.

[23] SLD Collaboration, SLAC-PUB-7629, contributed paper to EPS-HEP-97, Jerusalem, **EPS-122**;
SLD Collaboration, SLAC-PUB-7630, contributed paper to EPS-HEP-97, Jerusalem, **EPS-123**;
SLD Collaboration, contributed paper to EPS-HEP-97, Jerusalem, **EPS-124**;
SLD Collaboration, SLAC-PUB-7595, contributed paper to EPS-HEP-97, Jerusalem, **EPS-126**;
E. Etzion, talk presented at EPS-HEP-97, Jerusalem, to appear in the proceedings.

[24] ALEPH Collaboration, D. Buskulic *et al.*, Z. Phys. **C62** (1994) 179;
ALEPH Collaboration, D. Buskulic *et al.*, Phys. Lett. **B384** (1996)414;
ALEPH Collaboration., D. Buskulic *et al.*, *Measurement of the semileptonic b branching ratios from inclusive leptons in Z decays*, Contributed Paper to EPS-HEP-95 Brussels, **eps0404**.
This note may be found at http://alephwww.cern.ch/ALPUB/oldconf/HEP95/HEP95.html.

[25] ALEPH Collaboration, *Measurement of the partial decay width of the Z into $c\bar{c}$ quarks* contributed paper to ICHEP96, Warsaw, 25-31 July 1996 **PA10-016**. The results of the exclusive-exclusive and inclusive-exclusive double-tag D-meson measurements have been averaged for this note;
ALEPH Collaboration, *Study of Charmed Hadron Production in Z Decays,* contributed paper to the EPS-HEP-97, Jerusalem, **EPS-623**.

[26] DELPHI Collaboration, P.Abreu et al., Z. Phys. **C66** (1995) 323.

[27] DELPHI Collaboration, P.Abreu *et al.*, Z. Phys **C65** (1995) 569;
DELPHI Collaboration, P.Abreu *et al.*, Z. Phys **C66** (1995) 341;
DELPHI Collaboration, *Measurement of the Forward-Backward Asymmetries of* $e^+e^- \rightarrow Z \rightarrow b\overline{b}$ *and* $e^+e^- \rightarrow Z \rightarrow c\overline{c}$, DELPHI 95-87 PHYS 522.
This and all other Delphi notes are available at http://wwwcn.cern.ch/~pubxx/www/delsec/delnote/.

[28] L3 Collaboration, O. Adriani *et al.*, Phys. Lett. **B292** (1992) 454;
L3 Collaboration, M. Acciarri *et al.*, Phys. Lett. **B335** (1994) 542;
L3 Collaboration, *Measurement of* $R_{\rm b}$ *and BR(*$\rm b \rightarrow \ell X$*) from b-quark semileptonic decays,* L3 Note 1449, July 16 1993;
L3 Collaboration, *L3 Results on* $A_{\rm FB}^{\rm b\bar{b}}$, $A_{\rm FB}^{\rm c\bar{c}}$ *and* χ *for the Glasgow Conference,* L3 Note 1624;
L3 Collaboration, *L3 Results on* $R_{\rm b}$ *and* $\rm BR(b \rightarrow \ell)$ *for the Glasgow Conference,* L3 Note 1625;
L3 Collaboration, M. Acciarri *et al.*, Z Phys. **C71** 379 (1996);
L3 Collaboration, *Measurement of the* $e^-e^- \rightarrow Z \rightarrow b\bar{b}$ *Forward-Backward Asymmetry Using Leptons,* L3 Note 2112, contributed paper to the EPS-HEP-97, Jerusalem, **EPS-490**;
L3 Collaboration, *Measurement of the* $B^0 - \bar{B}^0$ *Mixing Parameter,* L3 Note 2113, contributed paper to the EPS-HEP-97, Jerusalem, **EPS-490**.

[29] OPAL Collaboration, G. Alexander *et al.*, Z. Phys. **C70** (1996) 357;
OPAL Collaboration, R. Akers *et al.*, *Updated Measurement of the Heavy Quark Forward-Backward Asymmetries and Average B Mixing Using Leptons in Multihadronic Events*, OPAL Physics Note PN226 contributed paper to ICHEP96, Warsaw, 25-31 July 1996 **PA05-007**
OPAL Collaboration, R. Akers *et al.*, *QCD corrections to the bottom and charm forward-backward asymmetries* OPAL physics note PN284.

[30] DELPHI Collaboration, *Measurement of the semileptonic b branching ratios and* $\bar{\chi}_b$ *from inclusive leptons in Z decays,* DELPHI 97-118 CONF 100 contributed paper to the EPS-HEP-97, Jerusalem, **EPS-415**.

[31] L3 Collaboration, O. Adriani *et al.*, Phys. Lett. **B307** (1993) 237.

[32] ALEPH Collaboration, R. Barate *et al.*, Physics Letters **B 401** (1997) 150;
ALEPH Collaboration, R. Barate *et al.*, Physics Letters **B 401** (1997) 163.

[33] DELPHI Collaboration, *Measurement of the partial decay width* $R_b^0 = \Gamma_{b\bar{b}}/\Gamma_{had}$ *with the DELPHI detector at LEP* , DELPHI 97-106 CONF 88, contributed paper to the EPS-HEP-97, Jerusalem, **EPS-419**.

[34] L3 Collaboration, *Measurement of the Z Branching Fraction into Bottom Quarks Using Double Tag Methods,* L3 Note 2114, contributed paper to the EPS-HEP-97, Jerusalem, **EPS-489**.

[35] OPAL Collaboration, K. Ackerstaff *et al.*, Z. Phys. **C74** (1997) 1.

[36] L3 Collaboration, *Afb(bb) using a jet-charge technique on 1994 data,* L3 Note 2129.

[37] OPAL Collaboration, R. Akers *et al.*, Z. Phys. **C67** (1995) 365.
OPAL Collaboration, *Measurement of the b quark forward-backward asymmetry around the Z0 peak using jet charge and vertex charge*, CERN PPE/97-06.

[38] DELPHI Collaboration, *Summary of R_c measurements in DELPHI,* DELPHI 96-110 CONF 37 contributed paper to ICHEP96, Warsaw, 25-31 July 1996 **PA01-060**.

[39] OPAL Collaboration, K. Ackerstaff *et al.*, CERN-PPE/97-093, Submitted to Zeit. Phys. C.

[40] ALEPH Collaboration, D. Buskulic *et al.*, Z. Phys. **C62** (1994) 1;
ALEPH Collaboration, D. Buskulic *et al.*, *The Forward–Backward Asymmetry for Charm Quarks at the Z pole: an Update*, Contributed Paper to EPS-HEP-95 Brussels, **eps0634**.
This note may be found at http://alephwww.cern.ch/ALPUB/oldconf/HEP95/HEP95.html.

[41] OPAL Collaboration, CERN-PPE/96-101 24 July 1996.

[42] D. Bardin *et al.*, Z. Phys. **C44** (1989) 493; Comp. Phys. Comm. **59** (1990) 303; Nucl. Phys. **B351**(1991) 1; Phys. Lett. **B255** (1991) 290 and CERN-TH 6443/92 (May 1992).

[43] The LEP Heavy Flavour Group, *QCD Corrections to $A_{\rm FB}^{\rm b\bar{b}}$ and $A_{\rm FB}^{\rm c\bar{c}}$ Measurements at LEPI*, LEPHF/97-01, ALEPH 97-081 PHYSIC 97-071, DELPHI 97-131 PHYS 720, L3 Note 2154, OPAL Technical Note TN500, 18 August 1997.

[44] ALEPH Collaboration, D. Decamp *et al.*, Phys. Lett. **B259** (1991) 377.

[45] ALEPH Collaboration, ALEPH-Note 93-041 PHYSIC 93-032 (1993);
ALEPH Collaboration, ALEPH-Note 93-042 PHYSIC 93-033 (1993);
ALEPH Collaboration, ALEPH-Note 93-044 PHYSIC 93-035 (1993).

[46] ALEPH Collaboration, D. Buskulic *et al.*, Z. Phys. **C71** (1996) 357.

[47] DELPHI Collaboration, P. Abreu *et al.*, Phys. Lett. **B277** (1992) 371.

[48] DELPHI Collaboration, *Measurement of the Inclusive Charge Flow in Hadronic Z Decays,* DELPHI 96-19 PHYS 594.

[49] L3 Collaboration, *Forward-Backward charge asymmetry measurement on 91-94 data*, L3 Note 2063.

[50] OPAL Collaboration, P. D. Acton *et al.*, Phys. Lett. **B294** (1992) 436.

[51] OPAL Collaboration, OPAL Physics Note PN195 (1995).

[52] T. Sjöstrand, Comp. Phys. Comm. **82** (1994) 74.

[53] G. Marchesini *et al.*, Comp. Phys. Comm. **67** (1992) 465.

[54] WW Cross-sections Working Group, W. Beenacker (convenor), F.A. Berends (convenor), *et al.*, "WW Cross-sections and Distributions", in *Physics at LEP2*, edited by G. Altarelli, T. Sjöstrand and F. Zwirner (CERN, Geneva, 1996), CERN 96-01, vol. 1.

[55] ALEPH Collaboration, R. Barate, *et al.*, Phys. Lett. **B401** (1997) 347.

[56] DELPHI Collaboration, P. Abreu, *et al.*, Phys. Lett. **B397** (1997) 158.

[57] L3 Collaboration, M. Acciarri, *et al.*, Phys. Lett. **B398** (1997) 223.

[58] OPAL Collaboration, K. Ackerstaff, *et al.*, Phys. Lett. **B389** (1996) 416.

[59] M. Rijssenbeek, talk presented at ICHEP96, Warsaw, 25-31 July 1996, to appear in the proceedings.

[60] LEP Energy Group, "LEP Energy Calibration in 1996", LEP Energy Group/97-01.

[61] D. Bardin, *et al.*, *GENTLE/4fan v. 2.0: A Program for the Semi-Analytic Calculation of Predictions for the Process* $e^+e^- \to 4f$, DESY 96-233, hep-ph/9612409.

[62] ALEPH Collaboration, *Measurement of the W-pair cross secin in* e^+e^- *collisiosn at 172 GeV*, CERN-PPE/97-102, submitted to Phys. Lett. B; ALEPH Collaboration, *W mass measurement through direct reconstruction in ALEPH*, contributed paper to EPS-HEP-97, Jerusalem, **EPS-600**.

[63] DELPHI Collaboration, *Measurement of the W-pair cross-section and of the W mass in* e^+e^- *interactions at 172 GeV*, DELPHI 97-108 CONF 90, contributed paper to EPS-HEP-97, Jerusalem, **EPS-347**.

[64] L3 Collaboration, M. Acciarri, *et al.*, *Measurement of W-Pair Cross Sections in* e^+e^- *Interactions at* $\sqrt{s} = 172$ *GeV and W-Decay Branching Ratios*, CERN-PPE/97-67, to be published in Phys. Lett. B;
L3 Collaboration, M. Acciarri, *et al.*, *Measurements of Mass, Width and Gauge Couplings of the W Boson at LEP*, CERN-PPE/97-98, submitted to Phys. Lett. B.

[65] OPAL Collaboration, *Measurement of the Mass of the W Boson Mass and Decay Properties in* e^+e^- *Collisions at* $\sqrt{s} = 172$ *GeV*, OPAL Physics Note PN301.

[66] SLD Collaboration, P. Rowson, talk presented at Moriond 97.

[67] CHARM II Collaboration, P. Vilain *et al.*, Phys. Lett. **B335** (1994) 246.

[68] S. Eidelmann and F. Jegerlehner, Z. Phys. **C67** (1995) 585.

[69] Y.K. Kim, talk presented at the Lepton-Photon Symposium 1997, Hamburg, 28 July - 1 Aug, 1997, to appear in the proceedings.

[70] CDHS Collaboration, H. Abramowicz *et al.*, Phys. Rev. Lett. **57** (1986) 298;
CDHS Collaboration, A. Blondel *et al.*, Z. Phys. **C45** (1990) 361.

[71] CHARM Collaboration, J.V. Allaby *et al.*, Phys. Lett. **B177** (1986) 446;
CHARM Collaboration, J.V. Allaby *et al.*, Z. Phys. **C36** (1987) 611.

[72] CCFR Collaboration, K. McFarland, *A Precision Measurement of Electroweak Parameters in Neutrino-Nucleon Scattering*, FERMILAB-Pub-97/001-E, January 1997, submitted to Phys. Rev. Lett.

[73] CDF Collaboration, J. Lys, talk presented at ICHEP96, Warsaw, 25-31 July 1996, to appear in the proceedings.

[74] DØ Collaboration, S. Protopopescu, talk presented at ICHEP96, Warsaw, 25-31 July 1996, to appear in the proceedings.

[75] The CDF and DØ results have been averaged together assuming a 3 GeV common systematic error.

[76] UA2 Collaboration, J. Alitti *et al.*, Phys. Lett. **B276** (1992) 354.

[77] CDF Collaboration, F. Abe *et al.*, Phys. Rev. Lett. **65** (1990) 2243 and Phys. Rev. **D43** (1991) 2070.

[78] CDF Collaboration, F. Abe *et al.*, Phys. Rev. Lett. **75** (1995) 11 and Phys. Rev. **D52** (1995) 4784.
A. Gordon, talk presented at XXXIInd Rencontres de Moriond, Les Arcs, 16-22 March 1997, to appear in the proceedings.

[79] DØ Collaboration, S. Abachi *et al.*, Phys. Rev. Lett. **77** (1996), 3309;
K. Streets, talk presented at Hadron Collider Physics 97, Stony Brook, to appear in the proceeedings.

[80] R.M. Barnett, *et al.*, Phys. Rev. **D54** (1996) 1.

[81] *Reports of the working group on precision calculations for the Z resonance*, eds. D. Bardin, W. Hollik and G. Passarino, CERN Yellow Report 95-03, Geneva, 31 March 1995.

[82] Electroweak libraries:
ZFITTER: see Reference 42;
BHM (G. Burgers, W. Hollik and M. Martinez): W. Hollik, Fortschr. Phys. **38** (1990) 3, 165; M. Consoli, W. Hollik and F. Jegerlehner: Proceedings of the Workshop on Z physics at LEP I, CERN Report 89-08 Vol.I,7 and G. Burgers, F. Jegerlehner, B. Kniehl and J. Kühn: the same proceedings, CERN Report 89-08 Vol.I, 55;
TOPAZ0: G. Montagna, O. Nicrosini, G. Passarino, F. Piccinnii and R. Pittau, Nucl. Phys. **B401** (1993) 3; Comp. Phys. Comm. **76** (1993) 328.
These computer codes have recently been upgraded by including the results of [81] and references therein.

[83] T. Hebbeker, M. Martinez, G. Passarino and G. Quast, Phys. Lett. **B331** (1994) 165;
P.A. Raczka and A. Szymacha, Phys. Rev. **D54** (1996) 3073;
D.E. Soper and L.R. Surguladze, Phys. Rev. **D54** (1996) 4566.

[84] See, for example, A. Czarnecki and J. Kühn, Phys. Rev. Lett. **77** (1996) 3955;
G. Degrassi, P. Gambino and A. Sirlin, Phys. Lett. **B394** (1997) 188.

[85] M. L. Swartz, Phys. Rev. **D53** (1996) 5268.

[86] A.D. Martin and D. Zeppenfeld, Phys. Lett. **B345** (1994) 558.

[87] H. Burkhardt and B. Pietrzyk, Phys. Lett. **B356** (1995) 398.

[88] R. Alemany, *et al.*, *Improved Determination of the Hadronic Contribution to the Muon* $(g-2)$ *and to* $\alpha(m_Z)$ *Using new Data from Hadronic* τ *Decays*, LAL 97-02, Feb 1997.

[89] J.P. Martin, *Higgs Particle Searches at LEP*, talk presented at ICHEP96, Warsaw, 25-31 July 1996, to appear in the proceedings.